GERMAN - MONGOLIAN INSTITUTE
FOR RESOURCES AND TECHNOLOGY

The present work was submitted to
the German-Mongolian Institute of Resources and Technology

TEMPORAL AND SPATIAL TRENDS OF FOREST FIRES AND CARBON DYNAMICS IN TUJIIN NARS

Bachelor's Thesis

by

ENKHJARGAL Batgerel

Study program: Environmental Engineering

Student ID: B2200214

1st Supervisor/Examiner: Prof. Dr. Gantuya Ganbat

2nd Supervisor/Examiner: Dr. Batsaikhan Vanchindorj

Advisor: Ms. Enkhjin Enkhbold

Ulaanbaatar/Nalaikh

2026

Statutory Declaration

Batgerel Enkhjargal	B2200214
Last Name, First Name	Student ID Number

I hereby affirm in lieu of an oath that I provided the submitted bachelor thesis

TEMPORAL AND SPATIAL TRENDS OF FOREST FIRES AND CARBON DYNAMICS IN TUJIIN NARS

I did not use any sources other than those stated. In case that the work is additionally submitted on a data medium, I declare that the written and the electronic form are completely identical. The work was not submitted in the same or similar form to any examination authority.

29.05.2026	
Place, Date	Signature

Acknowledgment

I wish to express my deepest thanks and gratitude to my supervisors, Prof. Dr. Gantuya Ganbat of German-Mongolian Institute for Resources and Technology and Dr. Batsaikhan Vanchindorj, Assistant Professor of the National Emergency Management Agency for their excellent mentorship, critical thinking and continuous support. Their expertise and constructive guidance on various aspects of this thesis are truly appreciated

My special thanks go to my advisor, Ms. Enkhjin Enkhbold for her unwavering support, invaluable insights and keen guidance throughout this thesis. Her encouragement and collaboration with regards to the technical details of the research were of great benefit

My gratitude is also extended to the teachers and staff of the Faculty of Raw Materials and Environmental Engineering of GMIT, who provided outstanding learning experience and abundant knowledge throughout my studies, creating the perfect academic environment for carrying out research.

Last, but by no means least, I would like to thank my family and friends for their unconditional love, understanding and encouragement, which provided me with strength and courage through the difficulties faced during the completion of this research project.

Abstract

Wildfires are one of the most important disturbances in boreal and forest steppe ecosystems, and are of great importance to biodiversity, carbon cycling and ecosystem resistance. In this study, a spatiotemporal analysis of wildfire dynamics, risks, emissions and post-fire carbon uptake in Selenge Province and the Tujiin Nars State Special Protected Area of northern Mongolia from 2001–2025 were performed. Wildfire occurrence and area burned are derived from the MCD64A1 burned area product processed by Google Earth Engine with verification data from the National Emergency Management Agency (NEMA) of Mongolia. LST, precipitation, wind speed, NDVI, slope, elevation and aspect were incorporated for fire risk and carbon calculation. During the period of this study (2001-2025) 605 fire detections and 7,809.29 km of burned area are detected in Selenge Province with maximum in 2009 (1,566.46 km) which shows peak fire year. Fire season is dominantly in Spring (March-May, 53% of total area burned) followed by Summer (37%). While in Tujiin Nars, fire occurs in three years of 2005, 2007 and 2025 with maximum burned area occurring in 2005 (83.633 km) followed by 2025 (41.383 km) and 2007 (36.684 km). Most fires were observed in north and northeast of the protected area, which coincides with distribution of forest steppe vegetation and environmental gradients. Wildfire risk was evaluated using multi criteria Wildfire Risk Index (RI) considering combustibility index, topomorphological index, human occupation index, and MaxEnt approach modeling species distribution. For provincial scale, prediction performance of MaxEnt model is highly satisfactory; LST becomes dominant factor in May (43.22%), and wind speed in October (42.88%), while precipitation is consistently important throughout the study season. Locally in Tujiin Nars the main contributing environmental variables controlling fire ignition varied with fire years, moisture and topographic factors controlled the fire in 2005 fire season; extreme thermal environment was a direct driver in 2007 fire season; while wind becomes the direct dominant driving factor for fire in 2025 fire season, which contributes 62.81% of the model and has permutation importance of 72.41%. All of the MaxEnt models have high performance in predicting fire occurrences with AUC values ranged from 0.836 to 0.966. The calculation of CO 2 emission from the fire events in Tujiin Nars was based on IPCC 2006 Guidelines, and despite that the cumulative burned area is mainly grasslands/steppes (160.37 km of 166.39 km in total, which accounts for 96.38% of total burned area), forest fire contribution to total CO 2 emission was 88.8% (5,706.96 out of 6,426.57 tons), which was 2,000,000 kg/km of fuel load compared with grassland (2,940 kg/km) of fire. And, the results of ecosystem recovery and carbon sequestration over years (from 2005 to 2025 based on MODIS GPP data) suggest a great recovery potential

of Tujiin Nars ecosystem, where mean C sequestration over year increases from 4.80 t C/ha to 6.26 t C/ha, and the total sequestration increased from 340,251.89 ton to 443,327.84 ton in 2025. These findings highlight the importance of fire prevention and ecosystem-based management for the carbon sequestration function and integrity of the Tujiin Nars State Special Protected Area under the context of climate change.

Keywords: Wildfire risk, MaxEnt modeling, Tujiin Nars, Selenge Province, MODIS burned area, Forest-steppe ecosystem, Spatiotemporal analysis

Table of Contents

1. Introduction 1

1.1 Objective 3

2. Methodology 4

2.1. Study area 4

2.2. Data 6

2.3. Methods 7

2.3.1 Wildfire Risk Index (RI) calculation 7

2.3.2 Maximum Entropy Fire Risk Analysis 11

2.3.3 Carbon emission estimation 13

2.3.4 Carbon Sequestration 14

3. Results and Discussion 15

3.1 Temporal and spatial distribution of wildfires in Selenge Province 15

3.2 Temporal and spatial distribution of wildfires in Tujiin Nars forest 21

3.3 Risk Index 23

3.4 MaxEnt Analysis 25

3.4.1 Analysis of Selenge 26

3.4.2 Analysis of Tujiin Nars 33

3.5 Carbon emission 43

3.6 Carbon sequestration 44

Conclusion 45

Reference 47

Appendix 49

List of figures

Figure 1. Distribution of State Protected Areas in Mongolia 2
Figure 2.Classification and extent of SPA in Mongolia 3
Figure 3.(a) Location map of Selenge Province (b) and the land cover distribution 4
Figure 4.Geographic location of the study area 5
Figure 5. Spatial distribution of environmental variables in Tujiin Nars 11
Figure 6.Fire history and burned area in Selenge Province from 2001 to 2025 16
Figure 7.Monthly and seasonal burned area patterns in Selenge Province from 2001 to 2025 16
Figure 8.Comparison of monthly wildfire incidents in Selenge Province from 2001 to 2025 17
Figure 9.Spatial distribution of forest fire frequency in Selenge Province from 2001 to 2025 18
Figure 10.Monthly wildfire fire counts and total burned area in Selenge Province 19
Figure 11. Monthly burned area in Tujiin Nars during recorded wildfire years (2005, 2007, and 2025) 21
Figure 12.Wildfire Frequency Map of Tujiin Nars (2001-2025) 22
Figure 13. Interannual variation of monthly mean LST, wind speed, and precipitation in Tujiin Nars during May-July (2001-2025) 23
Figure 14. a)Combustibility Index and b) Topomorphological Index map 25
Figure 15. Risk Index map of Tujiin Nars 25
Figure 16. Receiver Operating Characteristic (ROC) curve for the May wildfire model 26
Figure 17. Response of wildfire occurrence to environmental variables in May 28
Figure 18. Receiver Operating Characteristic (ROC) curve for the October wildfire model 29
Figure 19. Response of wildfire occurrence to environmental variables in October 30
Figure 20. Wildfire risk model from March to October across 2001 to 2025 32
Figure 21. Receiver Operating Characteristic (ROC) curve for the wildfire model in 2005 33
Figure 22. Response of wildfire occurrence to environmental variables in 2005 35
Figure 23. Receiver Operating Characteristic (ROC) curve for the wildfire model in 2007 36
Figure 24. Response of wildfire occurrence to environmental variables in 2007 37
Figure 25. Receiver Operating Characteristic (ROC) curve for the wildfire model in 2025 38
Figure 26. Response of wildfire occurrence to environmental variables in 2025 40

Figure 27. Comparison of environmental variable importance for wildfire occurrence in Tujiin Nars 42
Figure 28. Wildfire risk distribution in Tujiin Nars for 2005, 2007, and 2025 derived from the MaxEnt model 43
Figure 29. Carbon sequestration capacity of Tujiin Nars across wildfire years (2005, 2007, and 2025) 44

List of Tables

Table 1. NDVI-based Combustibility Classification 8
Table 2. Topomorphological Classification 9
Table 3. Human Occupation Classification 9
Table 4. Annual wildfire incidence and burned area in Tujiin Nars forest (2001-2025) 21
Table 5. Relative importance of environmental variables for wildfire occurrence in May 27
Table 6. Relative importance of environmental variables for wildfire occurrence in October 29
Table 7. Comparison of environmental variable importance for wildfire occurrence in Tujiin Nars (2005, 2007, 2025) 41
Table 8. Spatial distribution of carbon sequestration in Tujiin Nars for 2005, 2007, and 2025 43

1. Introduction

Wildfires are the dominant natural hazard influenced by the combined interaction of climate conditions, topography, fuels composition and ignitions by both nature and people. Wildfire is one of the global-scale ecological process and disturbance agents on ecological renewal and succession that controls biogeochemical cycles, community composition and biodiversity at regional to global scales. Given climate change, such recent decades have seen ever-increasing occurrences of severe climatic anomalies such as high temperatures, prolonged droughts and irregular precipitation. Increasing arid conditions throughout mid to high latitude regions are among others factors contributing to increased frequency and extent of wild fires, fire duration and intensity. This affects ecological functions like ecosystem nutrients cycles, energy flows and structure of landscape, reducing vegetation productivity and altering the habitat over large regions, posing major hazards to human beings, property and ecological resources. Over continent scales, wildfire activity has exhibited an upward trend in the Mongolian Plateau in association with the wider-trend toward climatically-enhanced wild fire in semiarid and boreal areas where there were warmer longer spring and autumn with less and shorter snow period and frequent hot events. The increased frequency of warm events has fueled easier ignition spread and larger fire size. This results in forest and steppe ecosystem damage, increased carbon emission and negative effect to pastoral communities where the economy relies on productivity of grassland. Emission of greenhouse gas and aerosols from combustion also is part of wider-climate feedback issue.

In Mongolia, management of Special Protected Areas (SPAs) is part of both the conservation of biodiversity and risk management from environmental factors. Currently, around 20.8% of the whole land area is under the SPA system with the aim to mitigate the impact of human pressures and tackle the problems of degrading ecosystems and environments linked to global climate change (Figure 1). SPAs conserve critical habitat, ensure ecosystem integrity and protect threatened species and plants. Furthermore, SPAs improve ecosystem resilience through restriction on unsustainable land uses and uncontrolled resource consumption, and promote adaptation to growing threats such as wild fires, desertification and biodiversity loss.

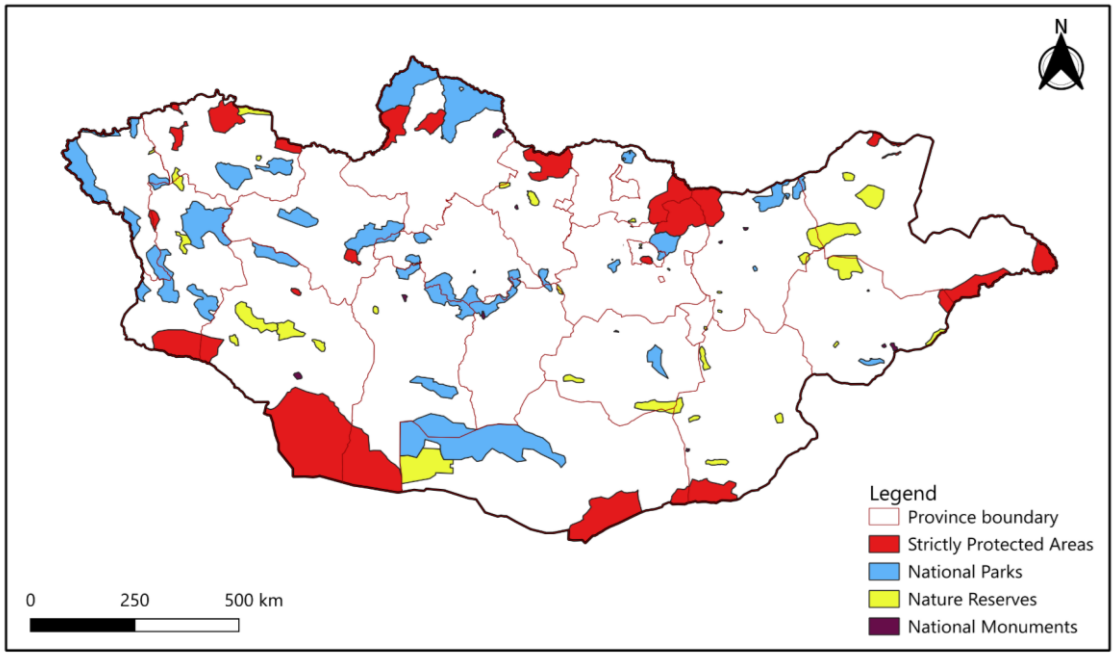


Figure 1. Distribution of State Protected Areas in Mongolia

Through the 1994 Law on Special Protected Areas, the system of national conservation management used for land protection in Mongolia was institutionalized. The Law defined four categories of management, described with respect to ecological value, importance to conservation and degree of human impact (Figure 2), thereby defining levels of land use permitted in various zoned areas. The law provided a legal basis for achieving conservation objectives while facilitating use of resources. These classifications are approximate to the International Union for Conservation of Nature (IUCN) protected areas categories. The incidence of wildfires is rising within SPAs as there is currently over 105 million ha of the fragile forest-steppe ecosystem in Mongolia protected for its high values as an SPA.

Most wildfires are thought to be anthropogenically caused as is evident from traditional pasturage practices (deliberately setting grassland on fire etc), and under existing climate change scenarios, fires will likely increase with continuing drought, temperature increases and greater wind speeds, causing additional pressures in terms of the degradation of habitats, loss of biodiversity, erosion and reduction of ecological resilience.

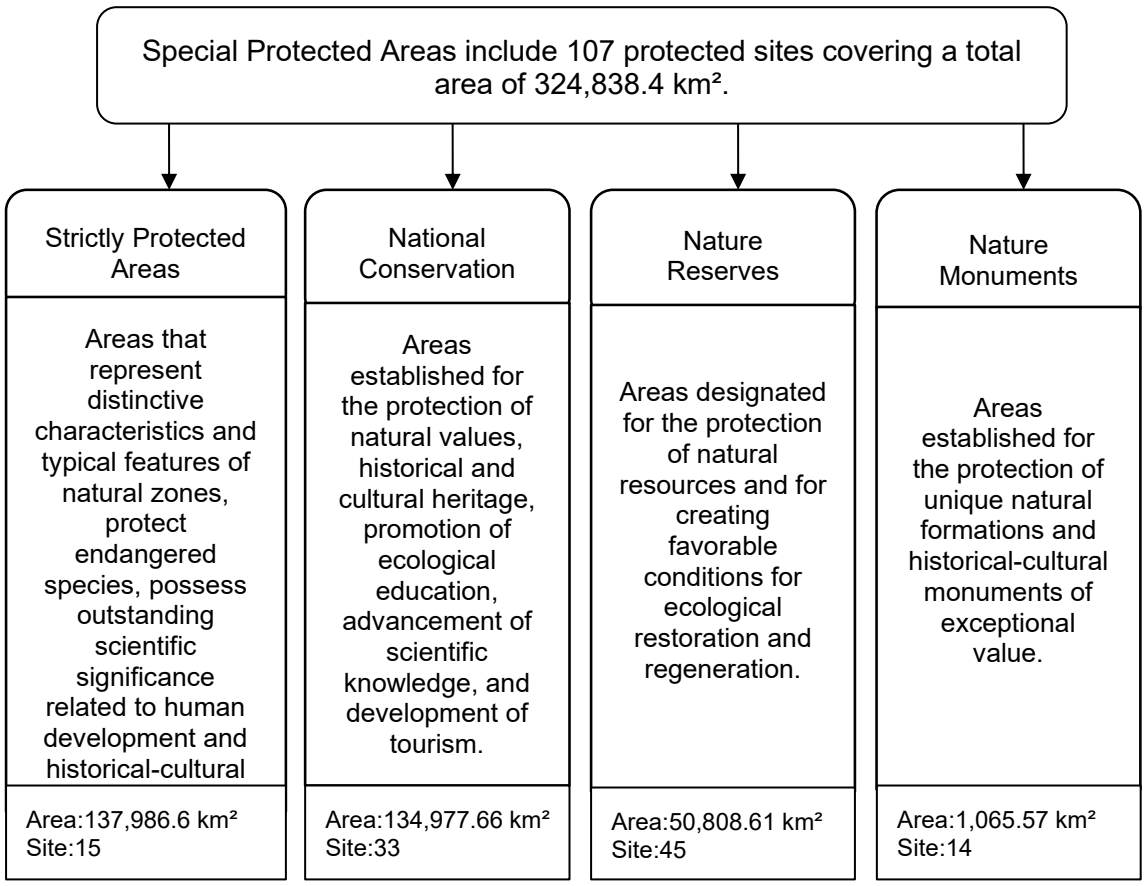


Figure 2.Classification and extent of SPA in Mongolia

1.1 Objective

The goal of this study is to conduct a comprehensive spatiotemporal analysis of wildfires in Selenge Province and the Tujiin Nars protected area for the period 2001-2025, and to assess wildfire risk, carbon emissions, and ecological impacts using satellite data and geospatial tools. The specific objectives are:

1. To map spatiotemporal wildfire patterns in Selenge Province and Tujiin Nars (2001-2025) using MODIS and geospatial tools.
2. To identify wildfire hotspots and seasonal trends in Selenge Province and Tujiin Nars through spatial clustering and time-series analysis.
3. To model wildfire risk using MaxEnt and environmental variables (temperature, wind, slope, NDVI, precipitation).
4. To estimate carbon emissions from wildfires in Tujiin Nars using IPCC-based calculations and burned-area data.
5. To assess post-fire changes in vegetation and carbon storage and evaluate wildfire impacts on ecosystem functions and environmental value.

2. Methodology

2.1. Study area

Selenge province is located in northern Mongolia. It extends approximately between 49°26' N latitude and 101°28' E longitude, bordering Russia to the north (Figure 3). This zone is located in a transition area between the mixing of Lake Baikal highland and the northern mountain system and the Mongolia Plateau. The function of this province in overall ecosystem is that its coniferous and deciduous forest is an area where soil protection, control over water and maintaining of permafrost can be achieved. As 66% of Selenge river basin area is in Mongolia and in the Selenge province more than 42% of land consists of forests and together with pasture land and cultivated land the province carries high environmental significance as well as an economical value. In the province high continental climate with long cold winters and short warm summers is found. Summer (June-August) temperature at 29.5°C-43°C and winter (December-February) at –35.6°C - –46.7°C are calculated based on the data provided by the Meteorological institute of Mongolia. Mean annual precipitation ranges from 93.5 to 273.5 mm with most of them concentrated in the summer. During April-July the wind force reaches its maximum, soil temperature is above 30C in summer and drops to –30°C- –35°C in December and January.

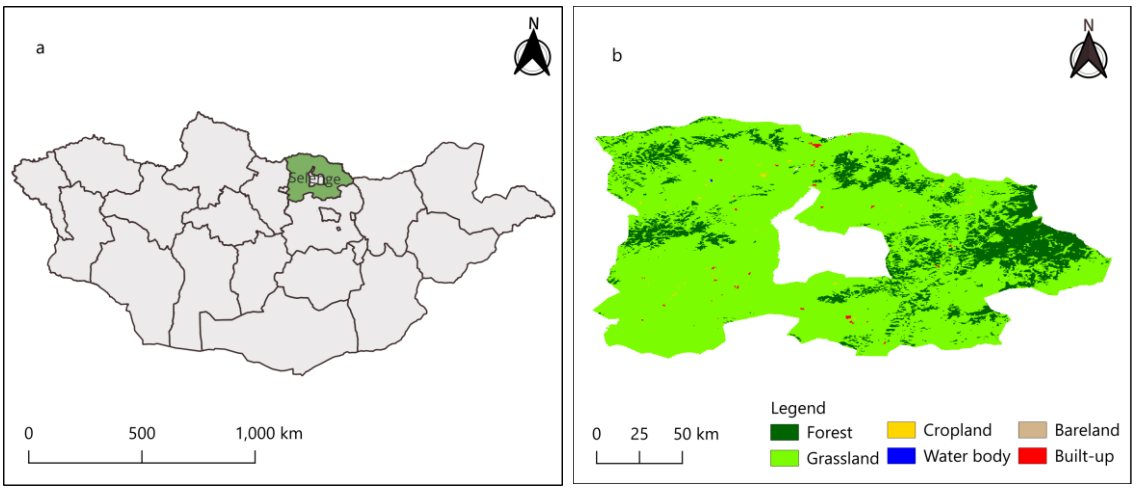


Figure 3.(a) Location map of Selenge Province (b) and the land cover distribution

Tujiin Nars is located in Altanbulag and Shaamar soums of Selenge Province (Figure 4). The territory represents native Scots pine (Pinus sylvestris) standing at the southeastern boundary of the Siberian boreal taiga and at the forest-steppe ecotone of Mongolia.

Thus, the Tujiin Nars becomes the connecting zone between the forest ecosystems and arid steppe environments of Central Asia due to its geographical position.

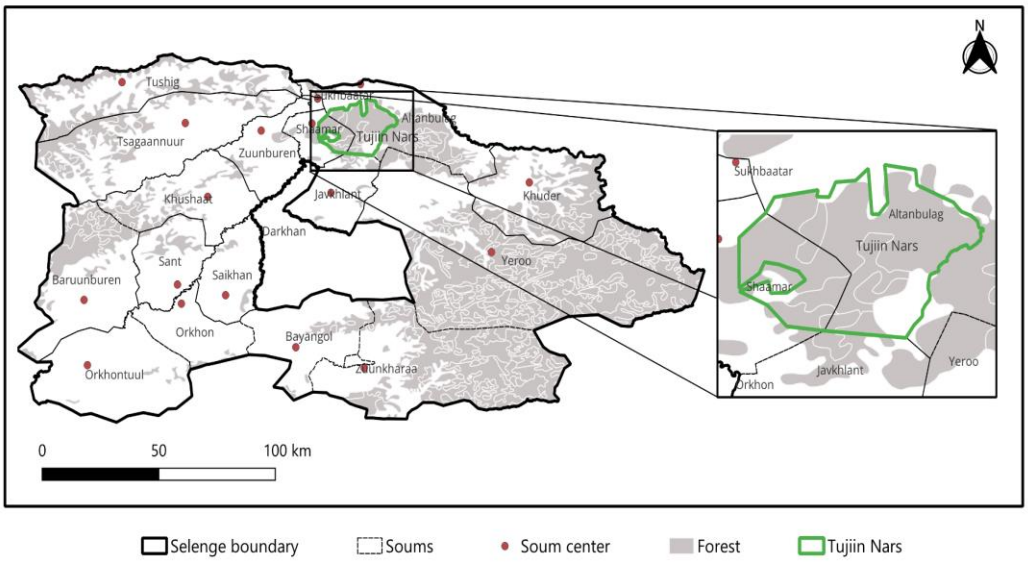


Figure 4.Geographic location of the study area

Historically, Tujiin Nars has been severely impacted by both natural and human-induced disturbances. Major wildfires in 1965, 1969, and 1990, together with unsustainable logging during the 1990s, caused substantial forest degradation and reduced ecosystem resilience. The ecological significance of the area was acknowledged by the Government of Mongolia, and it was designated as State Special Protected Area (Resolution #39 of State Great Khural, 2002) under the name of Tujiin Nars State Special Protected Area. The protected territory currently encompasses 65,548.56 ha and includes forest stands, steppe vegetation, sandy landscapes, and riverine ecosystems.

A large-scale reforestation program for burned wildfire areas was implemented right after that in 2003. The first stage of the project was a reforestation project of burned areas using Scots pine (Pinus sylvestris) seedlings, and it lasted from 2003 to 2014[5,6]. Over the project duration, plantation areas expanded from 100 ha in 2003 up to 350 ha in 2008 with 3,250 ha restored with 10.13 million trees and more being planted overall. This period has seen barren burned areas become young forest plantations and has proved to be one of Mongolia's largest-scale reforestation projects. The second stage of the program was launched in 2015 with management of plantation (tending, pruning, plantation improvement) rather than tree planting, which continued until 2014. Since 2015 over 600 ha of restored forest has been treated and has its conditions managed for improving survival and ecosystem quality until 2021. In 2021, the third stage has begun; establishing a research forest for ecological monitoring, climate change

adaptation and prevention of desertification. Tujiin Nars has become one of the good examples of a long-term forest rehabilitation of the former burned area [7].

2.2. Data

This study aims to describe and discuss the spatial and temporal characteristics of wildfires using both satellite remote sensing data and official wildfire records. The main burned area data were taken from the MODIS burned area product (MCD64A1 Version 6.1), which was processed using Google Earth Engine, representing monthly global burned area at a spatial resolution of 500m for the period 2001-2025. In order to confirm the results from remote sensing data, the statistics and official wildfire records were obtained from the Mongolian Statistical Service [8] and National Emergency Management Agency [9]. Furthermore, the other parameters including NDVI, land surface temperature, precipitation, wind speed and slope, were also processed using Google Earth Engine to perform fire distribution analysis.

In temporal analysis annual, monthly and seasonal trends were implemented to find behaviors at that time during the period of 2001 and 2025. Monthly MODIS burned area images were processed in Google Earth Engine and aggregated to obtain the yearly total burned area (km) and number of wildfire occurrences. With the annual analysis, the peak and the least activity years were observed while the monthly analysis determined the months that wildfire events predominantly happen and seasonal analysis categorized events into four seasons such as spring, summer, autumn, winter and analyzed its characteristics. Meanwhile, the comparison between the satellite derived wildfire counts and the official statistics data from the Mongolian Statistical Information Service was made in order to show the consistence of them. Finally, the results are illustrated by different types of charts and time-series graph to reflect wildfire activities over a long period of time.

Spatial analysis was performed to determine how fires were distributed throughout the region, where they clustered, and in which areas hotspots were located. The burned areas in the MODIS MCD64A1 dataset were selected and processed to fire patches and fire centroid points in Google Earth Engine. The resulting spatial outputs were then mapped using GIS software. Burned area maps were generated to quantify land impacted by fires, while fire frequency maps were used to reveal frequently burned areas. Spatial analysis was critical for locating vulnerable wildfire zones.

Weather-related variables were extracted from Google Earth Engine using the Tujiin Nars region between the years of 2001 and 2025, concentrating on the wildfire season

each year from May through September. The input for the wildfire variables is comprised of wind speed and precipitation, which were obtained from ERA5-Land Monthly Aggregated, while the LST values were obtained from the MODIS MOD11A2 Version 6.1 8-day LST product. Wind speed was calculated from the values for 10 m u- and v-wind speed by using the vector magnitude formula. Precipitation (expressed in meters) was then converted to millimeters by multiplying by 1000, and the LST (expressed in Kelvins) was converted to Celsius using the MODIS scale factor of 0.02 [12]. The means of wind speed, precipitation, and LST values over the region of Tujiin Nars were calculated for each month and were exported as a CSV table.

2.3. Methods

2.3.1 Wildfire Risk Index (RI) calculation

Wildfire risk in the Tujiin Nars study area was assessed using a spatially explicit multi-criteria evaluation approach that integrates key environmental and anthropogenic factors influencing fire ignition and spread. The overall wildfire susceptibility was quantified through the Wildfire Risk Index (RI), which combines vegetation conditions, terrain characteristics, and human accessibility into a single composite indicator. This approach allows for the identification of areas with varying levels of fire risk based on the interaction of fuel availability, topographic controls, and human-induced ignition sources [10].

The RI was calculated as a weighted linear combination of three component indices: the Combustibility Index (CI), the Topomorphological Index (MI), and the Human Occupation Index (HI). These indices represent the primary drivers of wildfire dynamics in forest-steppe ecosystems. The mathematical formulation of the RI is given as [10]:

$$RI = 5CI + 2MI + 3HI \quad \text{(Equation 1)}$$

In this formulation, higher weights were assigned to CI to reflect the dominant role of vegetation and fuel conditions in controlling fire occurrence and intensity. The HI component was assigned moderate importance due to the strong influence of human activities as ignition sources, while MI was given a lower weight, as terrain primarily influences fire behavior rather than ignition. The resulting RI values provide a continuous measure of wildfire susceptibility, which was subsequently reclassified into discrete risk categories for interpretation and mapping.

Combustibility Index (CI)

The Combustibility Index (CI) was developed to represent the spatial distribution of fuel availability and vegetation density, which are critical factors controlling wildfire ignition and propagation [10]. In this study, CI was derived using satellite-based vegetation

indicators from Sentinel-2 imagery acquired during the peak growing season (May–August). This period was selected to capture maximum vegetation development and biomass accumulation, thereby providing an accurate representation of potential fuel load.

Vegetation conditions were quantified using the Normalized Difference Vegetation Index (NDVI), a widely used spectral index for assessing vegetation health and density.

The NDVI values were reclassified into four combustibility levels, representing increasing fuel load conditions (Table.1). Areas with low NDVI values correspond to sparse vegetation or bare surfaces with limited fuel, whereas high NDVI values indicate dense forest or shrub cover with substantial combustible material.

Table 1. NDVI-based Combustibility Classification

NDVI Range	Class	Description
< 0.30	1	Low combustibility (bare or sparse vegetation)
0.30 – 0.50	2	Moderate combustibility
0.50 – 0.70	3	High combustibility
> 0.70	4	Very high combustibility (dense vegetation)

This classification assumes that areas with higher vegetation density accumulate greater biomass, which increases the likelihood of ignition and supports more intense fire behavior. However, it is acknowledged that vegetation moisture content may also influence combustibility, which is not explicitly considered in this index.

Topomorphological Index (MI)

The Topomorphological Index (MI) was used to quantify the influence of terrain on wildfire behavior, particularly fire spread rate, direction, and intensity. Terrain characteristics play a critical role in wildfire dynamics by affecting fuel dryness, wind exposure, and heat transfer processes [10].

The MI was derived from a Digital Elevation Model (DEM) and incorporates three key topographic parameters: slope, aspect, and morphology. These parameters were classified into ordinal categories and combined using the following:

$$\mathrm{MI} = 3s + (m * a) \qquad \text{(Equation 2)}$$

where, s represents slope, m represents terrain morphology, and a represents aspect.

Slope influences the rate of fire spread, as fires tend to move more rapidly uphill due to preheating of fuels. Aspect determines the degree of solar radiation exposure, which affects fuel moisture conditions; south-facing slopes are generally drier and more

susceptible to burning. Morphology reflects broader terrain characteristics, such as valleys and ridges, which can either facilitate or hinder fire movement.

Each parameter was classified into four levels ranging from low to high influence, and the resulting MI values were reclassified into four categories representing increasing suitability for fire spread (Table.2).

Table 2. Topomorphological Classification

Class	MI	Description
1	0-5	Low (unfavorable for fire spread)
2	5-10	Moderate
3	10-15	High
4	15-25	Very high (favorable for fire spread)

Higher MI values indicate terrain conditions that enhance fire propagation, particularly in steep, sun-exposed areas.

Human Occupation Index (HI)

The Human Occupation Index (HI) represents the spatial influence of human activities on wildfire ignition. In forest-steppe environments, a significant proportion of wildfires are caused by anthropogenic factors, including transportation, grazing activities, and recreational use.

In the Tujiin Nars study area, permanent settlements are largely absent within the protected forest boundary. Therefore, human influence was primarily represented by road accessibility, which serves as a proxy for human presence and activity. A buffer-based approach was applied to capture the spatial extent of potential human impact.

A buffer distance of 1000 meters was generated around mapped road networks, assuming that areas within this distance are more likely to be affected by human activities. This threshold is commonly used in wildfire studies to represent zones of increased ignition probability.

Table 3. Human Occupation Classification

Condition	Class	Description
Outside buffer	1	Low human influence
Within 1000 m	2	High human influence

Table 3. Summary of spatial environmental variables, data sources, resolution, temporal coverage, and processing methods used in the study

Data	Source	Resolution	Period	Processing
NDVI	Sentinel-2 (COPERNICUS/S2_SR) / Landsat 5 (LT05)	10–30 m	May–August (2005,2007, 2021, 2025)	Cloud masking, radiometric scaling, NDVI calculation, percentile classification (p25, p50, p75)
DEM	NASADEM (NASA/NASADEM_HGT)	30 m	Static	Derivation of slope and aspect, elevation classification
Slope	Derived from DEM	30 m	Static	Classification into 4 classes (flat to steep)
Aspect	Derived from DEM	30 m	Static	Reclassification into directional classes (N, E, S, W)
Vegetation	ESA WorldCover / NDVI-based classification	10 m	2025	Reclassification into vegetation types (forest, grassland, etc.)

This approach reflects the assumption that wildfire ignition probability decreases with increasing distance from access routes.

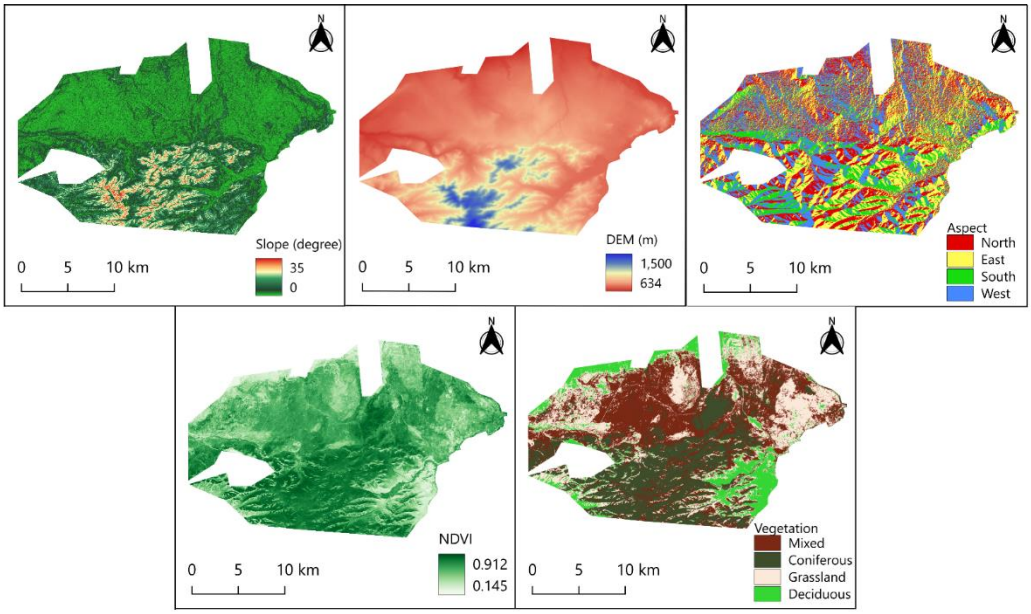


Figure 5. Spatial distribution of environmental variables in Tujiin Nars

2.3.2 Maximum Entropy Fire Risk Analysis

MaxEnt is the most commonly applied machine-learning algorithm for wildfire risk modeling, relying on presence-only data and associated environmental variables. It creates a predicted probability distribution of fire occurrence within the study area based on associating fire locations with existing environmental conditions such that predicted values match recorded ones. The MaxEnt model requires the input of two key data-wildfire occurrences (X) and correlated environmental variables (Y), both need to be at the same resolution level.

If we denote the wildfire occurrence data as X = (x_1, x_2, ..., x), the information entrop f X can be calculated as:

$$H(x) = -\sum_i^n \; p(x = x_i) log(x = x_i) = -\sum_i^n \; p(X)\; log(X) \qquad \text{(Equation 3)}$$

As the wild fire distribution X depends on the environmental factor Y, we can define a training sample set (X|Y) by overlaying the wild fire occurrence points and the environmental data. When incorporating Y, the probability distribution and information entropy of X changes to a conditional entropy:

$$H(X|Y\,) = -\sum_n \quad p(X,Y)\; log(X,Y) \qquad \text{(Equation 4)}$$

The maxent model assumes that among all the possible probability distributions compatible with the known constraints, it is the probability distribution with the highest entropy which doesn't assume any unknown information i.e. the Maxent is the least

biased and most uniform predictions. To obtain: optimization of the objective function is performed by Maxent model,

$$X^* = argmax\ H(X,Y) \quad \text{(Equation 5)}$$

The parameters of the model are estimated with the method of maximum entropy, using the technique of random seeds, which makes sure that the predicted values are closer to the observed ones. The model accuracy is evaluated using training and test samples. Since the result may be varied due to randomness, we take an average value of a certain number of runs.

To estimate the prediction accuracy of the Maxent-based fire risk model, we utilized the receiver operating characteristic (ROC) curve and area under the ROC curve (AUC). The ROC curve plots true positive rate (sensitivity) versus false positive rate (1-specificity) at different classification thresholds applied to the Maxent output, and AUC combines the curve in a single scalar value. AUC value of 0.5 means random classification; any AUC above 0.5 suggests a discrimination above random level, while values greater than 0.8-0.9 often signify good-to-excellent prediction accuracy. In Maxent, AUC calculation normally involves fire presence sites and random background pseudoabsence locations and expressed as separate values for training and testing set when cross validation or random partitioning is used.

The Maxent model provides four main output formats that represent the same underlying fire-risk pattern but in different scales and interpretations:

- Raw: This is simply the raw, unscaled output from the Maxent model. It displays the relative suitability of a given location, presented as a continuous variable, though the variables are not bounded between 0 and 1, nor should they be considered probabilities. This raw data should only be used for internal diagnostics and for comparison.
- Cumulative: The cumulative results will change the raw suitability into percentiles. For any given location, the cumulative value of that location indicates the percentage of the study area that has suitability values lower than or equal to the specified location. This is best understood as an approximated omission rate threshold: if you set a threshold at 90%, the model predicts that ~10% of occurrence locations will fall below that threshold.
- Logistic: These are scaled the same as the raw results; except they are scaled between 0 and 1 by a sigmoid (S-shaped) function. This is what is commonly thought of as a probability-like variable for occurrence, though they are relative.
- Cloglog (complementary log-log): These are scaled like the logistic, between 0 and 1, but use a different equation that is best used when the structure and

sampling design looks like a rare event. Like logistic, these result in a 0-1 range and are generally the default output for the probability-like occurrence maps.

Logistic and cloglog outputs are usually more appropriate in wildfire risk mapping because the values are bounded from 0 to 1 and are easy to interpret. Outputs could also be reclassified into categories of risk (low, moderate, high and very high risk) using defined thresholds. In this study, the cloglog output was employed as a wildfire risk zone.

2.3.3 Carbon emission estimation

Carbon emissions from wildfires in Tujiin Nars were estimated using an IPCC-based bottom-up approach, which integrates burned area, fuel load, combustion completeness, and emission factors to quantify CO_2 emissions from biomass burning. The calculation follows:

$$E_{CO2} = A \times FL \times CC \times EF_{CO2} \quad \text{(Equation 6)}$$

Where:

- $E_{CO2}$is total CO_2 emission,
- A is burned area (km²),
- FL is fuel load (kg/km²),
- CC is combustion completeness,
- and EF_{CO2} is the emission factor (kg CO_2/kg biomass).

Burned area data were derived from the MODIS MCD64A1 burned area product using Google Earth Engine for three representative fire years: 2005, 2007, and 2025. Burned pixels were identified for the main fire season (May-July), and total burned area was calculated by summing pixel areas at 500 m resolution.

To improve emission estimates, burned areas were classified by land cover using the MODIS MCD12Q1 dataset. Land cover classes were grouped into forest and grassland/steppe, reflecting the forest-steppe transition characteristics of Tujiin Nars. This distinction is important because biomass availability and combustion behavior differ significantly between vegetation types.

Fuel load values were assigned based on literature-reported biomass ranges. A value of 2,000,000 kg/km² (20 t/ha) was used for forest areas, representing typical biomass density of temperate pine forests, while 2,940 kg/km² was used for grassland areas. Combustion completeness was assumed as 0.30 for forest and 0.95 for grassland, reflecting partial versus near-complete biomass consumption during fire events. Emission factors were set to 1.58 kg CO_2/kg biomass for forest and 1.613 kg CO_2/kg

biomass for grassland, consistent with reported values for temperate and boreal ecosystems [4].

Carbon emissions were calculated separately for each land cover type and then summed to obtain total emissions. All calculations were performed at the pixel level in Google Earth Engine, allowing spatially explicit estimation of wildfire-related CO_2 emissions.

2.3.4 Carbon Sequestration

Post-fire changes in vegetation condition and carbon sequestration in Tujiin Nars were assessed to evaluate the impact of wildfire on ecosystem functions and environmental value. The analysis focuses on how fire disturbance alters vegetation structure, productivity, and the capacity of the ecosystem to absorb atmospheric carbon.

Vegetation response to fire was analyzed using the Normalized Difference Vegetation Index (NDVI), which reflects vegetation density and photosynthetic activity. NDVI was calculated for the growing season before and after fire events, and the difference between these periods was used to identify areas of vegetation loss and subsequent recovery. Reduced NDVI values indicate fire-affected or degraded areas, whereas higher values suggest vegetation regeneration.

To further characterize fire impact, burn severity was evaluated using the differenced Normalized Burn Ratio (dNBR). This index allows classification of fire-affected areas into different severity levels, providing insight into the intensity of vegetation damage and its spatial distribution. Areas with high burn severity typically experience greater biomass loss and slower recovery rates.

Carbon sequestration was assessed using MODIS Gross Primary Productivity (GPP) data, which represents the amount of carbon fixed by vegetation through photosynthesis .Seasonal GPP values were aggregated to estimate the carbon uptake capacity of the ecosystem and to generate spatial patterns of sequestration. This approach enables identification of areas with high and low carbon absorption potential.

In the Tujiin Nars forest-steppe ecosystem, post-fire dynamics show clear spatial differences. Grassland and steppe areas generally recover rapidly due to fast-growing vegetation and show relatively high short-term carbon uptake. In contrast, forest areas exhibit slower recovery because fire affects not only canopy vegetation but also ground-level biomass such as litter, branches, and organic layers. As a result, carbon sequestration in forested areas is reduced immediately after fire and recovers gradually over time.

Overall, the integration of NDVI, dNBR, and GPP provides a comprehensive framework for assessing wildfire impacts. While fires result in immediate carbon loss, post-fire vegetation recovery plays a critical role in restoring ecosystem productivity and carbon sequestration capacity.

3. Results and Discussion

3.1 Temporal and spatial distribution of wildfires in Selenge Province

Figure 6 represents the annual fire occurrence and burn area in Selenge province from 2001 to 2025, using information derived from satellite data, statistical records, and official reports of NEMA. Annual fire occurrence and burnt area fluctuated very much throughout the period. Highest burn area was observed in 2009 with a total burned area of 1,566.46 km 2, followed by 2007 with 925.40 km 2 and 2008 with 885.44 km 2. In contrast, very small and/ or no burn area was detected in 2013, 2019, 2021-2023. Though statistical records and an official NEMA report revealed the existence of wild fires in 2021 and 2023, none burned area or fire event was found by the GEE based MODIS burn area product in the relevant years. There is a possible relationship between the burned area/fire event that was NOT detected and spatial resolution, fire size, fire duration, cloud/smoke influence, or operational reported fires not detected by MODIS. In comparison with the wildfire trend in eastern Mongolia, Selenge Province was exposed to lower wildfire impacts as compared to the hotspot provinces. In general, larger and more severe fires occur in Dornod, Khentii, and Sukhbaatar [22].
In the year 2025, data sources have the widest discrepancy between one another. Satellite was able to identify 36 fire events whereas the 2018-2025 statistical counts show approximately 100, and the official NEMA dataset shows 106 fire events making 2025 have the most reported fire incidents during the 2018-2025 study period. Interestingly, with the abnormally high number of reported fires in 2015, the total burned area for the 2015 fire incidents was only 390.44km, much less than major wildfire years in 2009, 2007, and 2008, implying a high number of reported fires does not necessarily mean a large area burned. By analyzing the 2018-2025 combined incident data, I identified that the 2015 data may have duplicate dates within the same soum (indicating the same fire event recorded several times) or very small short duration events and/or nearby hot spots within a large fire recorded individually; GEE data may have aggregated nearby burned areas into a single fire event. Overall, the 2015 data shows that fire incidents may lead to an overestimate of severity as the area burned was significantly smaller.

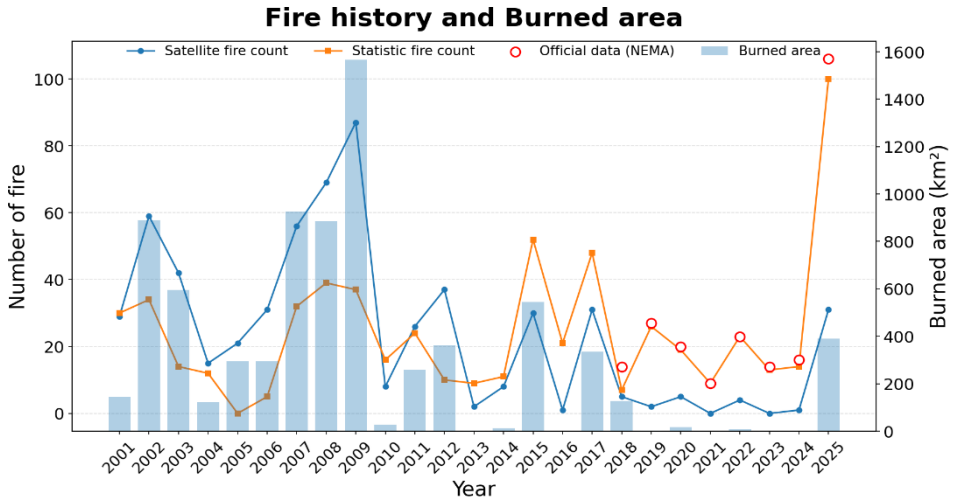


Figure 6.Fire history and burned area in Selenge Province from 2001 to 2025

Figure 7 shows monthly and annual distribution of burned area in Selenge Province over the period 2001–2025 from satellite data. The monthly examination shows that wildfire mostly happens in between April and September, with relatively strong spikes in May, June and July. A clear spike in monthly variation is seen in some years (e.g., during the late 2000s) with few intense burning months concentrated during a short time, whereas no, almost no burned area can be observed during January, February, November and December, with cold season wildfire being insignificant.

Seasonal breakdown confirmed that the spring was the major fire season (53%) in 2001-2025 with the largest portion of total burned area. Summer was the next largest fire season (37%) and autumn with about 10% of the total burned area. Winter was less than 1% of the total burned area. However, although the spring was the major fire season over the total period, there were few years in which the burning was dominated by summer and it showed the extended risk into the middle of summer if it continued the long period of drought and less precipitation.

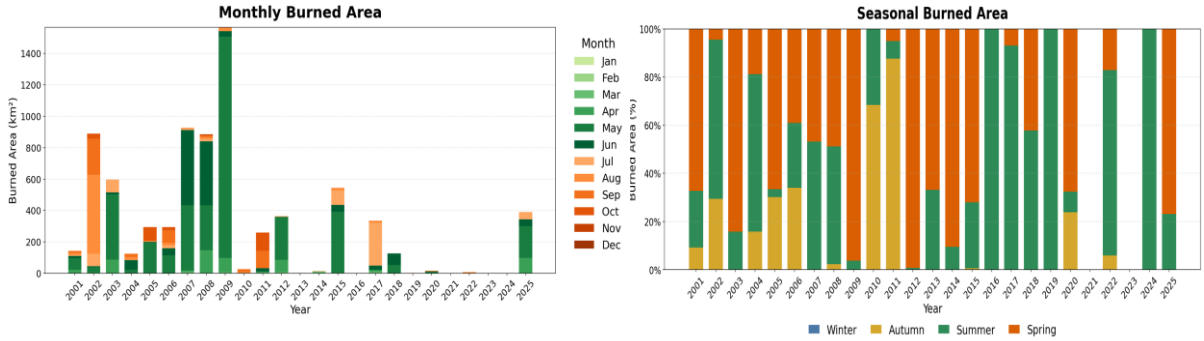


Figure 7.Monthly and seasonal burned area patterns in Selenge Province from 2001 to 2025

Figure 8 compares monthly distribution of wildfire in Selenge Province based on satellite annual fire data. Black line shows the monthly long term average fire frequency while the color lines represent the year. This figure demonstrated a distinct fire season with fires occurring between March and October and virtually no fires being registered between November and February. Higher levels of fire activity typically appeared in spring, especially in May, when monthly peaks were observed in most of the years and at the highest values for 2003 and 2009. Secondary surge was identified at late summer, fall season (August-October) with important peaks being observed for 2002 and 2011.

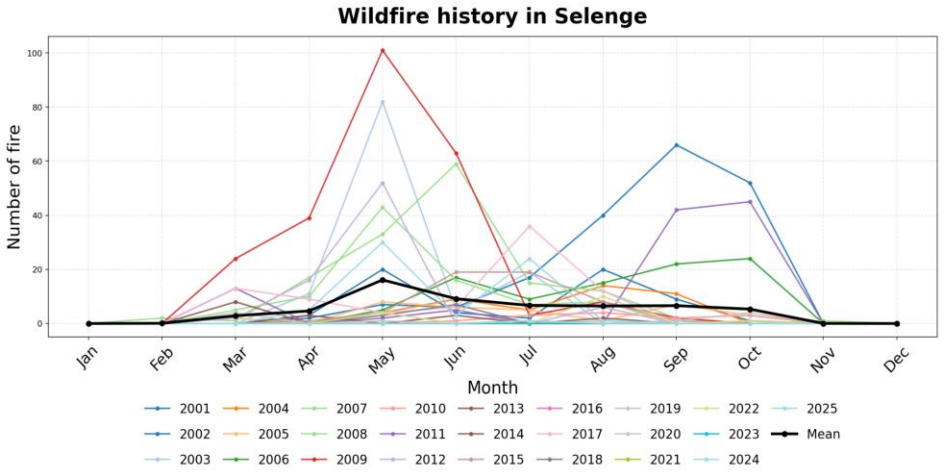


Figure 8.Comparison of monthly wildfire incidents in Selenge Province from 2001 to 2025

Figure 9 represents the cumulative number of fire detections across Selenge province over the period 2001-2025. The frequency was calculated from the MODIS Burned Area Product (MCD64A1 Version 6.1) at a resolution of 500 m utilizing GEE. Fire observations were extracted from MODIS monthly burned area products by selecting the fire occurrences inside the study region and BurnDate > 0 and extracting the burned pixels from all months. The fire pixels within forests (from MODIS Land Cover Product-MCD12Q1) were separated from all land types by using yearly land cover data. The frequency map was produced by accumulating all burned observations over time. Wildfires are clustered mainly in the northern, north-eastern, and eastern areas of Selenge province. Most parts of this area are close to the forest area of the borders and mountain land. High recurrence areas occurred mostly at local spot areas. Low recurrence rate (1-2 fires) was widely spread. Moderately high to high recurrence (6-14 fires) and very high recurrence (>15 fires) rate are only limited to a few spot areas.

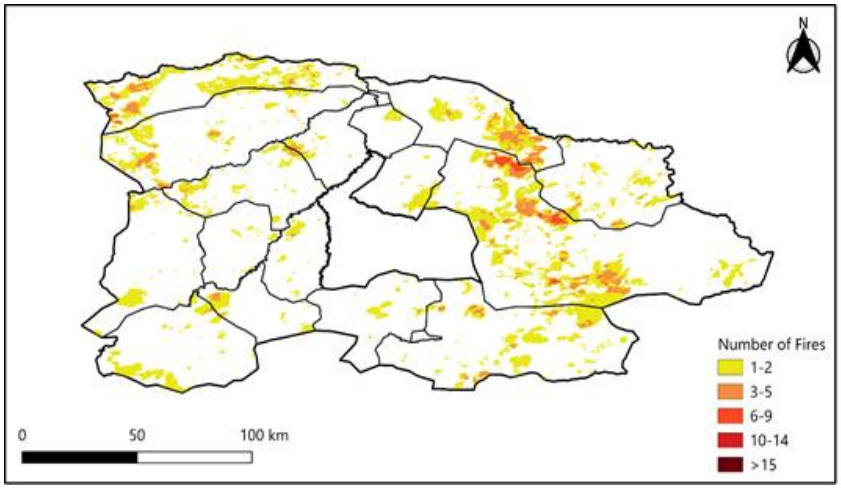


Figure 9.Spatial distribution of forest fire frequency in Selenge Province from 2001 to 2025

Figure 10 represents the annual and monthly number of fires along with the total burned area (km^2) in Selenge province from 2001 to 2025. Over the entire study period, there were 605 fire detections and the total burned area was 7,809.29 km^2. The number of annual fires was highest in 2009 (87 fires), followed by 2008 (69 fires) and 2007 (56 fires). Interestingly, there were no satellite-detected wildfire events in 2021 and 2023, while some official records report fire incidents during those years. The number of annual burned areas was highest in 2009 (1,566.46 km), followed by 2007 (925.40 km^2) and 2008 (885.44 km^2) and indicated that the late 2000s was the worst period for wildfire in the province. The burned areas in the recent few years were the lowest. The monthly distribution suggests that wildfire occurrences predominantly happen during April to September confirming the warm-season fire regime for the Selenge province.

Year	Jan	Feb	Mar	Apr	May	Jun	Jul	Aug	Sep	Oct	Nov	Dec	Total	Total Area (km²)
2001	0	0	0	3	18	1	1	3	3	0	0	0	29	143.797
2002	0	0	0	2	4	1	6	21	19	6	0	0	59	889.861
2003	0	0	0	7	26	2	7	0	0	0	0	0	42	595.96
2004	0	0	0	0	2	3	1	3	6	0	0	0	15	123.787
2005	0	0	2	0	11	2	0	0	0	6	0	0	21	293.952
2006	0	0	0	0	3	5	4	5	11	3	0	0	31	293.82
2007	0	0	1	5	33	11	5	1	0	0	0	0	56	925.399
2008	0	1	0	12	17	24	6	2	5	0	2	0	69	885.437
2009	0	0	5	22	54	5	0	1	0	0	0	0	87	**1566.461**
2010	0	0	0	0	0	0	1	3	4	0	0	0	8	27.313
2011	0	0	2	0	0	1	0	0	10	13	0	0	26	259.391
2012	0	0	2	11	24	0	0	0	0	0	0	0	37	363.3

2013	0	0	0	2	0	0	0	0	0	0	0	0	2	2.454
2014	0	0	8	0	0	0	0	0	0	0	0	0	8	13.553
2015	0	0	1	1	2	11	11	4	0	0	0	0	30	544.415
2016	0	0	0	1	0	0	0	0	0	0	0	0	1	0.165
2017	0	0	6	3	1	5	13	3	0	0	0	0	31	335.287
2018	0	0	0	0	1	4	0	0	0	0	0	0	5	126.427
2019	0	0	0	0	0	0	0	2	0	0	0	0	2	2.567
2020	0	0	0	0	2	0	2	0	0	1	0	0	5	16.775
2021	0	0	0	0	0	0	0	0	0	0	0	0	0	0.0
2022	0	0	0	0	0	0	0	4	0	0	0	0	4	8.412
2023	0	0	0	0	0	0	0	0	0	0	0	0	0	0.0
2024	0	0	0	1	0	0	0	0	0	0	0	0	1	0.322
2025	0	0	0	6	12	4	14	0	0	0	0	0	36	390.435
Total	**0**	**1**	**27**	**76**	**210**	**79**	**71**	**52**	**58**	**29**	**2**	**0**	**605**	**7809.29**

Figure 10. Monthly wildfire fire counts and total burned area in Selenge Province

3.2 Temporal and spatial distribution of wildfires in Tujiin Nars forest

The trend of annual wildfire occurrence and the corresponding burned area in Tujiin Nars forest using the GEE data during 2001-2025. The wildfire occurrences were found to be at three distinct years, 2005, 2007 and 2025, and the fires occurred infrequently within the study period. Between these years, wildfire intensity in 2005 was found to be highest, which contained 7 fire events and a total burned area of 83.633 km; the fires were burned in May (4 times) and June (3 times). While wildfire intensity was reduced to 2 fire events in 2007; the fires were burned in May, with a burned area of 36.684 km. However, wildfire intensity increased to 6 fire events in 2025; with one event burning in June, 5 events in July, and the burned area was 41.383 km, higher than 2007 though with the number of events close to 2007 (Table.4).

Year	May	June	July	Total	Total area, km^2
2005	4	3	0	7	83.633
2007	2	0	0	2	36.684
2025	0	1	5	6	41.383

Table 4. Annual wildfire incidence and burned area in Tujiin Nars forest (2001-2025)

The distribution of burned area per month throughout the years the study found wildfire is shown in Figure 11. It shows that the burned area was highest in May 2005 which is also the highest single fire month in the study time period. Another high burned area can be found in May 2007, this result further indicates that Spring season is prone to wildfire in this study area. Wildfires occurred much later in the year 2025 with most burned areas occurring in June and July.

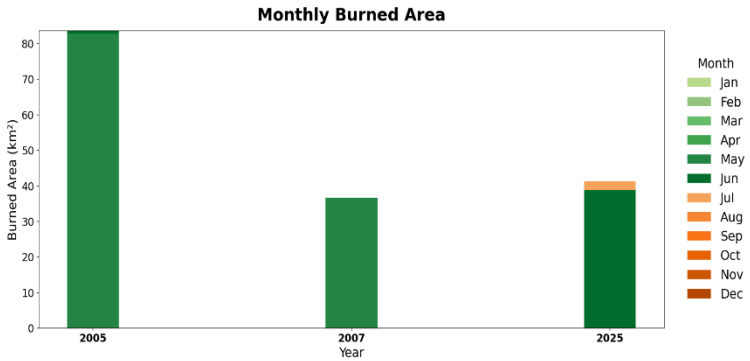


Figure 11. Monthly burned area in Tujiin Nars during recorded wildfire years (2005, 2007, and 2025)

Wildfire occurrence over the entire study period (2001-2025) for Tujiin Nars is shown in Figure 12. Wildfire frequency was categorized into four recurrence classes; no fire occurrence (0), single occurrence (1), frequent occurrence (2-3), and highest recurrence (4-5 fire occurrences). Low frequency wildfire occurrences constituted the major pattern with the vast majority of burned pixels having only a single fire occurrence. The areas prone to single occurrence wildfires primarily occupied the northern and northeastern forest zone, with a smaller portion located in the western section. Areas that experienced moderate fire recurrence (2-3 events) occurred mostly in the eastern region of Tujiin Nars. Areas prone to the highest recurrence (4-5 events) had only a single localized hotspot in the eastern region indicating extreme recurrence at that location. The central and southern regions of Tujiin Nars did not contain any recorded wildfire occurrences.

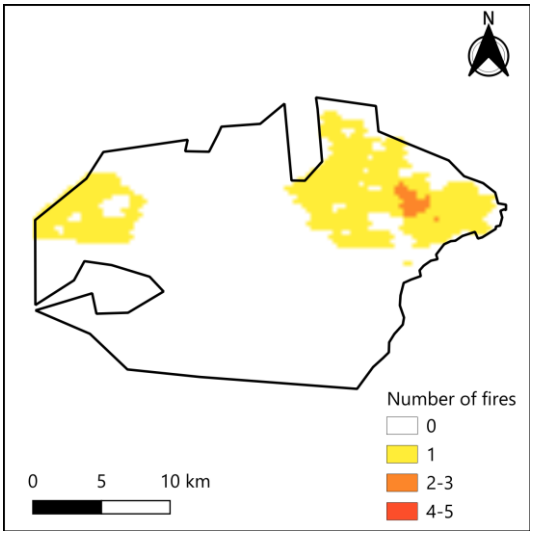
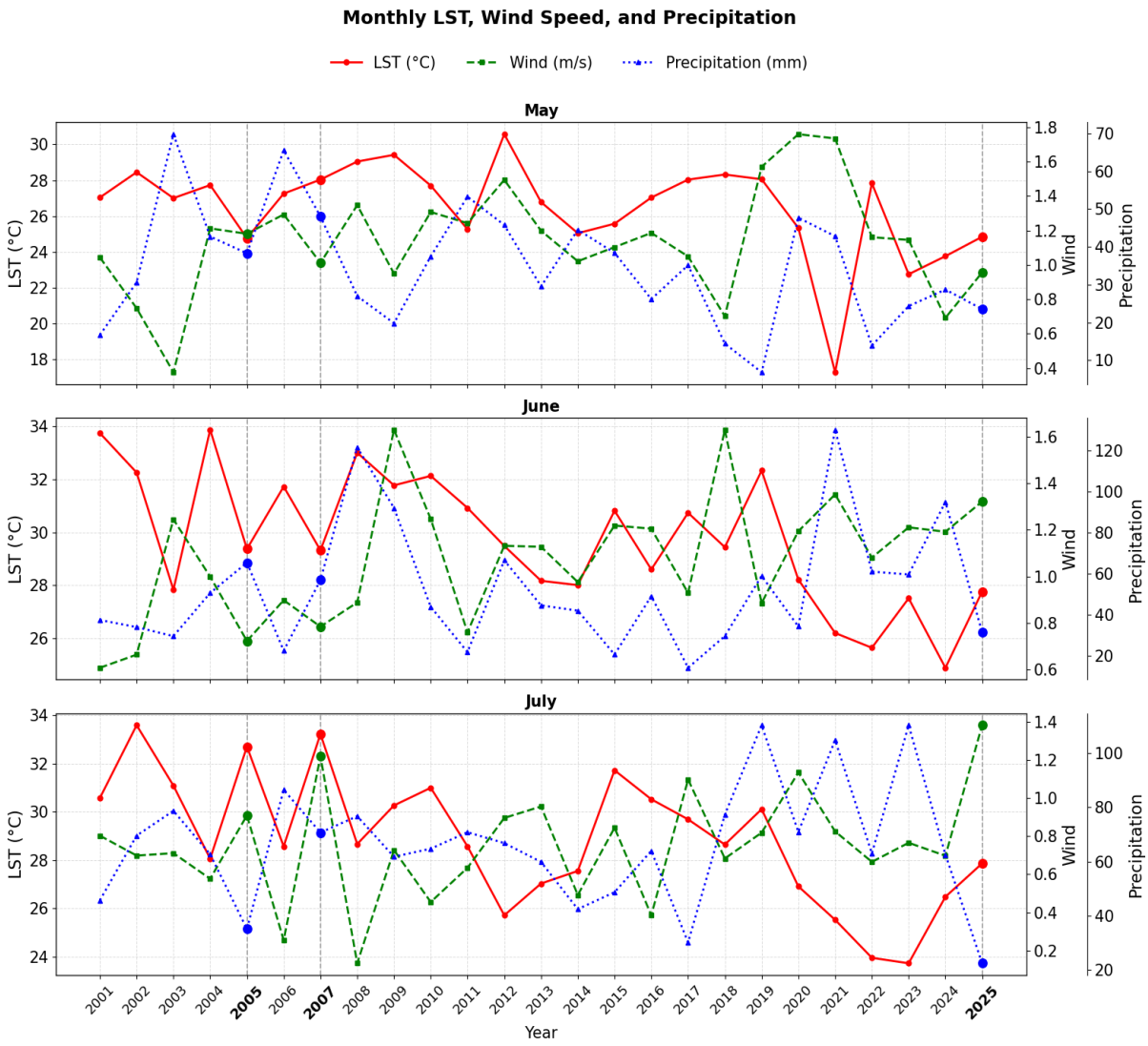


Figure 12.Wildfire Frequency Map of Tujiin Nars (2001-2025)

Interannual variability of May-July monthly mean land surface temperature (LST), wind speed, and precipitation in Tujiin Nars from 2001 to 2025 is depicted in Figure 11. High interannual variation was noted for all three environmental variables which probably contributes to the wildland fires in the area. Generally, the conditions that lead to fire are coupled with high temperature, low precipitation, and relatively strong wind speed. Highest LST occurred in May, June, and July, whereas precipitation values vary significantly with years. These values indicated warm and dry conditions early in summer probably coupled with stronger wind can enhance fire risk. In comparison of fire years to the monthly environmental condition revealed a more direct relation to the occurrence of wildfire years. In 2005 wildfires were in May and June instead of July. During the occurrence of wildfire, May was moderate in temperature (24.8°C), had relatively high wind speed (1.18 m/s), and moderate precipitation. June was hot in temperature (29.4°C) and low in wind speed and higher precipitation compared to May. This suggested that

high temperature and sufficient dry fuel in late spring to early summer are responsible for wildfire occurrence in 2005. In 2007, it seemed that the wildfire occurrence was influenced by high temperature and strong wind speed instead of drought conditions only. In 2025, which has official fire occurrences during late June to early July, has the least precipitation (22-31 mm) and highest wind speed (1.32-1.38 m/s), had the highest signal for environmental control of wildland fires. In general, fire occurrence in Tujiin Nars is highly dependent on the synergy between heat and seasonal drying wind conditions during the fire season.

Figure 13. Interannual variation of monthly mean LST, wind speed, and precipitation in Tujiin



Nars during May-July (2001-2025)

3.3 Risk Index

The spatial pattern of RI is primarily controlled by the Combustibility Index (CI), which reflects vegetation density and fuel availability derived from NDVI. As shown in Figure

14a, high and very high CI classes are mainly concentrated in the central and southern parts of the study area, where NDVI values are relatively high. These areas represent dense vegetation cover and increased biomass accumulation, resulting in higher fuel availability and greater wildfire susceptibility. In contrast, the northern and northeastern parts exhibit lower CI values, indicating sparse vegetation and reduced fuel load.

Terrain influence on wildfire behavior is represented by the Topomorphological Index (MI), which describes the effect of slope, aspect, and elevation on fire spread and intensity. As illustrated in Figure 14b, higher MI values are mainly observed in the central and southern mountainous regions, where steep slopes and favorable aspect conditions enhance fire propagation. These conditions promote faster fire spread through increased heat transfer and reduced fuel moisture. Conversely, flatter areas in the northern part of the study area show lower MI values, indicating less favorable conditions for wildfire spread.

The Human Occupation Index (HI) represents the influence of human activities, which are a major source of wildfire ignition. In this study, HI was derived from road accessibility, with higher values assigned to areas located within close proximity to roads. Although the spatial extent of HI is relatively limited compared to CI and MI, it locally increases wildfire risk along transportation corridors, highlighting the role of human presence in fire ignition.

The combined RI results indicate that high and very high-risk zones are predominantly concentrated in the central and southern parts of Tujiin Nars, where dense vegetation, favorable terrain conditions, and road accessibility overlap. In contrast, lower risk classes dominate the northern and northeastern areas, where vegetation density and terrain influence are relatively lower. These results demonstrate that vegetation conditions (CI) play a dominant role in determining wildfire risk, while terrain (MI) and human influence (HI) act as secondary factors that enhance fire spread and ignition at the local scale.

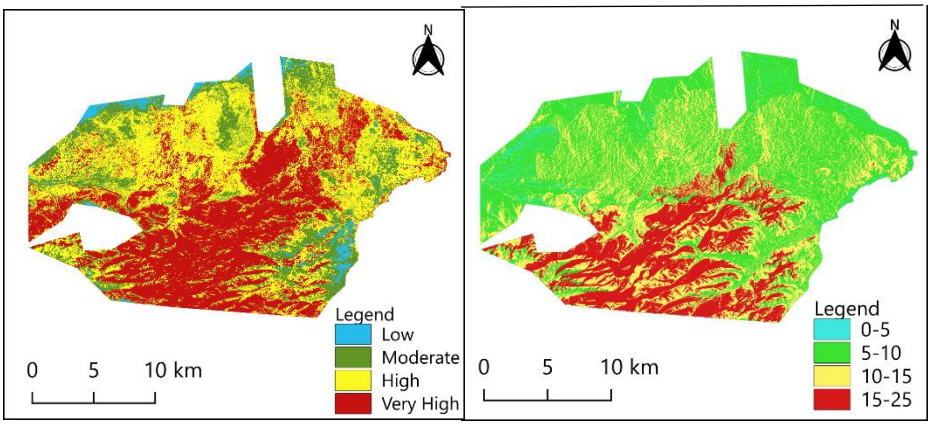


Figure 14. a)Combustibility Index and b) Topomorphological Index map

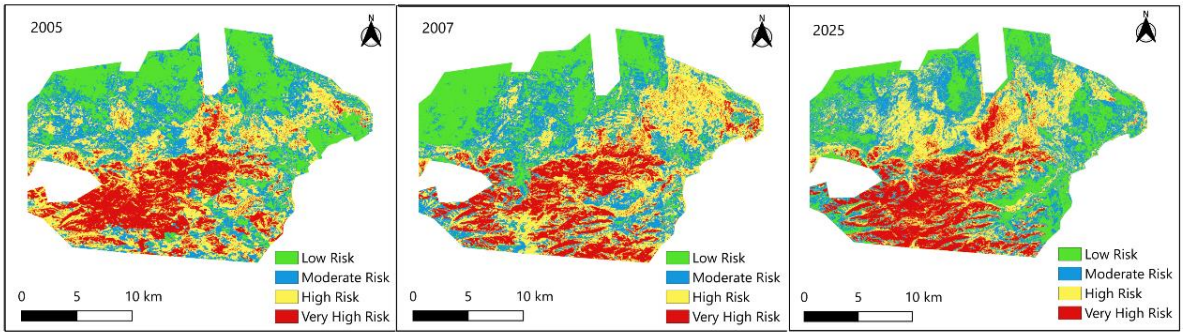


Figure 15. Risk Index map of Tujiin Nars

3.4 MaxEnt Analysis

Initially MaxEnt models were applied at provincial level to estimate spatial fire risk and to study the effect of environmental variables on a monthly basis in Selenge Province. Based on the past trend of fire occurrences in long-term, fire occurrence is concentrated in between months from March to October, thus analysis was conducted in these fire seasons only. From November to February there was no fire data to use as a presence, thus no models were generated for this period. Of the all-fire seasons month, May has been selected for detailed analysis and October as a typical low fire month as it is highly probable that wildfire can occur only during active months of fire and highest fire occurrences observed in October. For local application MaxEnt model was conducted in Tujiin Nars based on the fire occurrences for recorded fire years of 2005, 2007 and 2025 for central fire months like May, June and July and to explore variation of the environmental variables on wildfire occurrences in seasonal period and variable responses across months and years of different periods.

3.4.1 Analysis of Selenge

3.4.1.1 Performance of the model and environmental variable influence in May

A total of 2412 fire presence locations were used for the May MaxEnt model, where 80% of data was used for training the model and 20% randomly selected to test the model. The accuracy performance shows fairly adequate predictability; Training AUC = 0.743, Test AUC = 0.742.

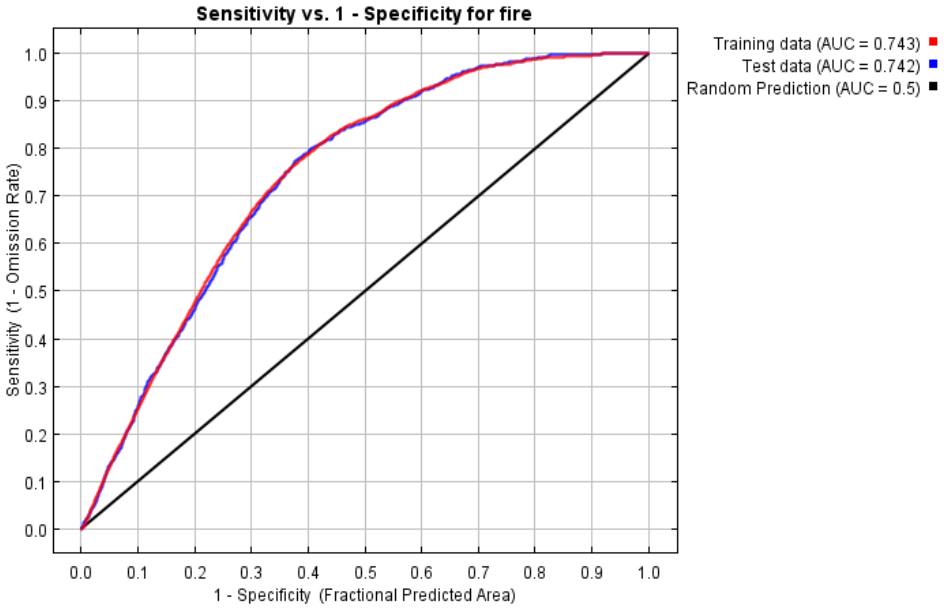


Figure 16. Receiver Operating Characteristic (ROC) curve for the May wildfire model

Five environmental variables were identified in the May wildfire risk model of Selenge province by MaxEnt analysis (Table.5). Land Surface Temperature (LST) was the most influential variable in the model with a 43.22% contribution, which reflects the importance of heat in forming wildfire hazardous circumstances. Precipitation had the second highest contribution at 27.28%, which showed the moisture deficit of May played an important role in raising the possibility of fire hazard. Wind Speed made a 14.92% contribution to the model which showed the influence on fire spreading. Both Slope and NDVI have relatively low contributions, which are 9.4% and 5.18% respectively. It indicates that these two factors did not have independent prediction power for the occurrence of May wildfire. From the comparison of contributing percentages, it can be seen that Land Surface Temperature and Precipitation have great influence on the wildfire occurrence and they accounted for over 70% of the entire model's contribution.

Table 5. Relative importance of environmental variables for wildfire occurrence in May

Variable	Contribution (%)	Permutation Importance (%)
LST	43.22	34.69
NDVI	5.18	13.36
Precipitation	27.28	30.62
Slope	9.4	2.87
WindSpeed	14.92	18.46

The response curves of MaxEnt are the result of plotting changes in the prediction of the probability of occurrence when each environmental variable is increased or decreased, but while the remaining variables are maintained at their average levels. The response curves used in this analysis are displayed in their original units, i.e., land surface temperature, precipitation, wind speed and slope (Figure 17), thus each can be interpreted directly.

- LST response is generally positive, indicating that as temperature increases above 20°C probability increases more or less monotonically, reaching a maximum between 30°C and 32°C and suggesting that as land surface temperature increases the conditions become favorable for the occurrence of wildfires.
- NDVI response is clearly non-linear with the probability of wildfire being very high when values of the vegetation index are low (0.30-0.35), dropping off considerably and a subsequent small spike around 0.50-0.55, suggesting that low density and moderately dense vegetation may pose a fire risk under dry conditions.
- Precipitation response indicates that the probability of wildfire is high under low precipitation, decreasing with increasing levels of precipitation, and that it acts as a crucial limiting factor for the occurrence of wildfire in May.
- Slope response is relatively flat across most degrees, although slightly positive at the highest slopes, suggesting a small positive response to fire occurrence at steep slopes.
- Wind speed has a clear maximum probability of wildfire around 0.70-0.80 m/s and subsequently drops off, only to rise again for values above that.

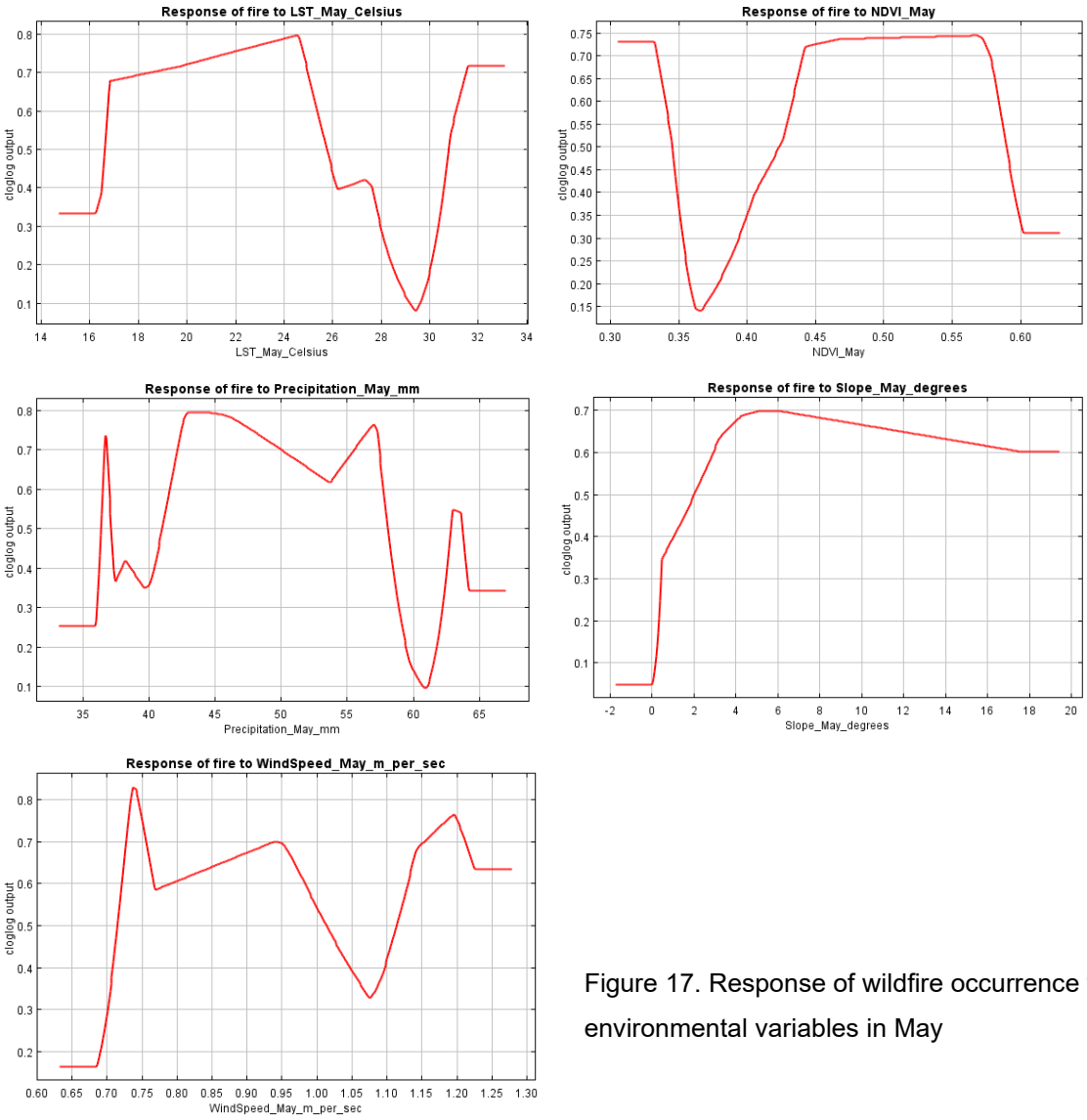


Figure 17. Response of wildfire occurrence to environmental variables in May

3.4.1.2 Performance of the model and environmental variable influence in October

The MaxEnt model for October showed strong predictive performance, with a training AUC of 0.897 and test AUC of 0.892, indicating excellent model reliability (Figure.18).

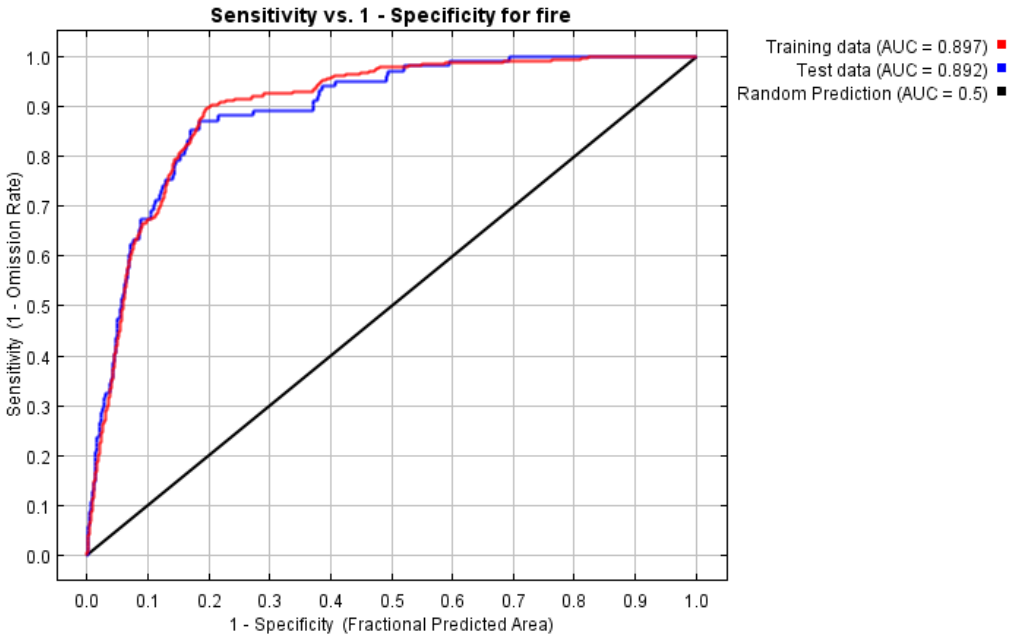


Figure 18. Receiver Operating Characteristic (ROC) curve for the October wildfire model

However, differently to May, October showed that wind speed was the most predictive variable contributing 42.88% with permutation importance of 47.04%, proving that fall wind conditions have significant control over fire hazard. LST provided a second contribution (22.06%), following precipitation (20.43%) which both account for thermal and humidity influences. Slope (7.47%) and NDVI (7.17%) appeared insignificant in terms of their contributions (Table.6).

Table 6. Relative importance of environmental variables for wildfire occurrence in October

Variable	Contribution (%)	Permutation Importance (%)
LST	22.06	14.89
NDVI	7.17	17.1
Precipitation	20.43	19.38
Slope	7.47	1.58
WindSpeed	42.88	47.04

The response curves show how wildfire probability in October relates to the varying environmental variables across the province of Selenge (Figure. 19).

- LST: fire probability increases as LST rises gradually above 20°C and has a maximum near 28-30°C (suitability 0.8) with a steep drop-off beyond 32°C. These characteristics indicate that moderate autumn temperature favors wildfires.

- NDVI: fire probability is maximized at low values of the vegetation index (0.30-0.35; suitability 0.9) with decreases at intermediate values and another small peak at values around 0.55-0.60. These patterns demonstrate that dry, sparse October vegetation encourages wildfires.
- Precipitation: fire probability is highest below 15 mm precipitation (suitability ~0.9) with abrupt decreases at over 20-25 mm. The patterns reiterate that drought in October is a trigger for wildfires.
- Slope: fire probability increases steadily from nearly 0.1 in flat terrain to over 1.0 above 14-15°C slope. This suggests that increasing steepness promotes October wildfires continuously.
- Wind Speed: fire probability rises fastest in response to this parameter from nearly 0.2 at 0.15 m/s to over 0.9 above 0.55-0.65 m/s and above that value up to 0.80 m/s. The patterns also reflect that Wind Speed has the most influence on fire probability for the October model.

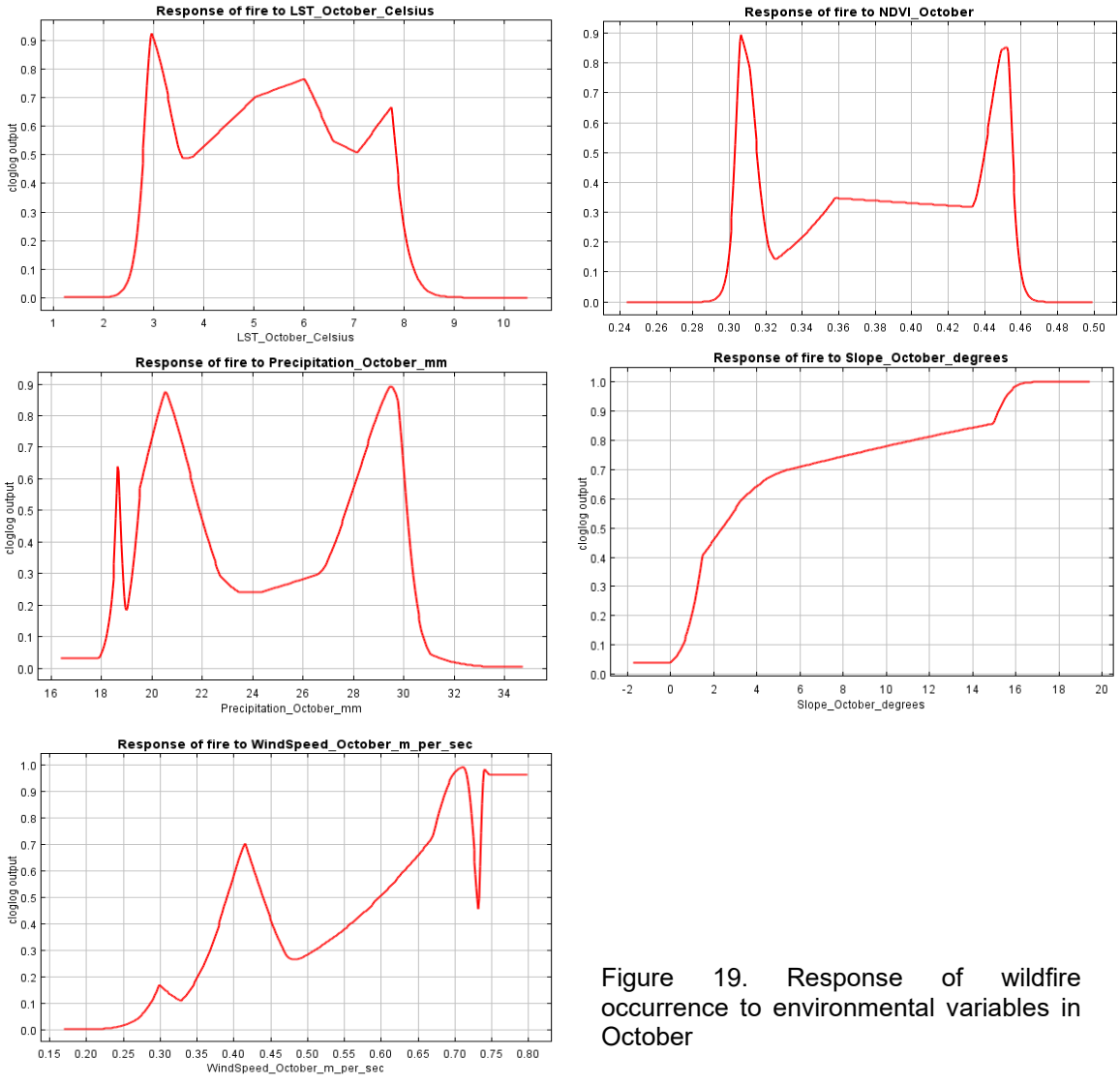


Figure 19. Response of wildfire occurrence to environmental variables in October

3.4.1.3 Comparison of environmental variable influence between May and October

The MaxEnt models for May and October revealed notable differences in the relative importance and response patterns of environmental variables driving wildfire risk in Selenge province.

- LST had the highest relative contribution in May with 43.22% and had a comparatively low relative contribution of 22.06% in October. However, in both months' response was always positive and fire probability was at peak when LST was in the range of 28-32°C, thus indicating LST still remained a significant fire predictor in both seasons although its contribution became low in autumn and other variables played their dominant role.
- Precipitation also exhibited a similar strong relation with the occurrence of fire in both the months (relative contribution of 27.28% in May and 20.43% in October; permutation importance of 30.62% in May and 19.38% in October). In both cases, fire probability was highest for extremely dry conditions thus, indicating that deficit precipitation is a non-seasonal and continuous fire predictor in Selenge.
- Wind speed was the most distinctive parameter among the predictor variables, as its relative contribution in October (42.88%) greatly increased as compared to its value in May (14.92%), and it was the strongest fire predictor in autumn. Also, the response curves confirmed this; it raised dramatically for high wind speed in October, as compared to May.
- NDVI played a minor role in both the months (relative contribution of 5.18% in May and 7.17% in October) however, its permutation importance value was slightly increased in October from 13.36% to 17.10%.
- Slope had consistently low values both for relative and permutation importance (in May relative contribution of 9.4% and permutation importance of 2.87% and in October relative contribution of 7.47% and permutation importance of 1.58%).

Thus, it is concluded that thermal driver LST played an important role in the early summer season whereas wind became a significant fire predictor for autumn. Precipitation was a strong fire predictor in both the months.

3.4.1.4 Wildfire Risk Modelling of each month

In Fig. monthly wildfire risk maps are presented for Selenge Province over the period 2001-2025.

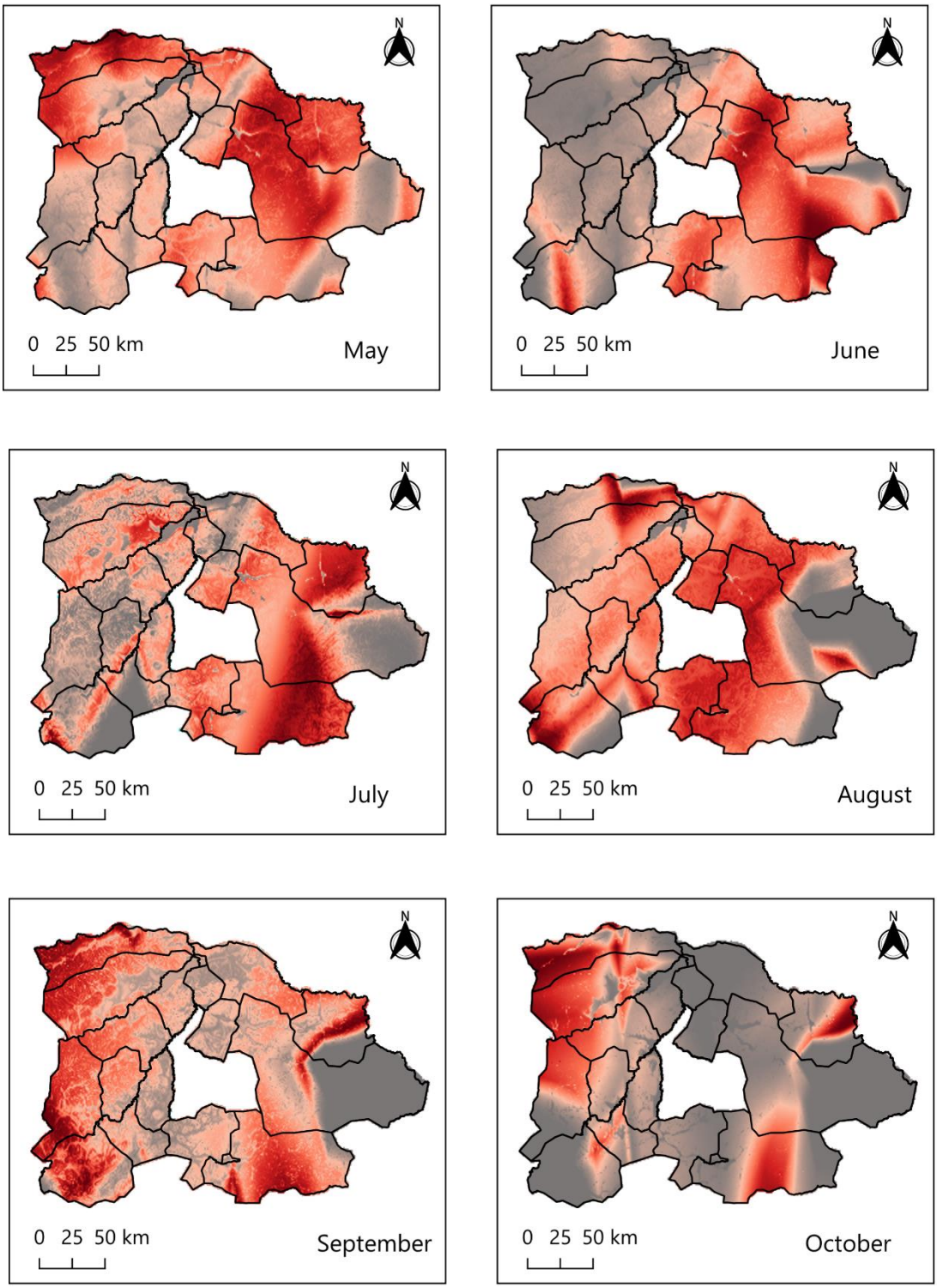


Figure 20. Wildfire risk model from March to October across 2001 to 2025

3.4.2 Analysis of Tujiin Nars

In this study, wildfire occurrence records from Tujiin Nars were used to run the MaxEnt model. There were relatively little occurrence data because of the limited spatial extent and occurrence scale of wildfire events in Tujiin Nars, and thus, the present-only strategy was used to conduct the analysis. One km thinning was implemented to remove spatial clumping and possible sampling bias in pixel-based occurrence data to ensure that only one point was within a 1km cell and then potential spatial autocorrelation and overfit of the models could be decreased. Even after thinning, the number of occurrences data were limited, and the data were randomly split into 80% training data and 20% testing data. Performance of the model was assessed using AUC index. High values for AUC index were obtained, and therefore, the accuracy of the model seems reasonable. However, the values of AUC with a small number of samples might overestimate the prediction capability, for there are few testing data when the occurrence numbers are limited. Although the prediction ability is well-indicated in AUC values, potential uncertainty and sampling bias might be present.

3.4.2.1 Performance of the model and environmental variable influence in 2005 (May-July)

The ROC curve demonstrates that the MaxEnt model performs with high predictive accuracy. The training dataset produced an AUC value of 0.911, while the test dataset yielded an AUC of 0.886. Since both values are significantly higher than 0.7, the model can be considered reliable and effective for wildfire risk prediction.

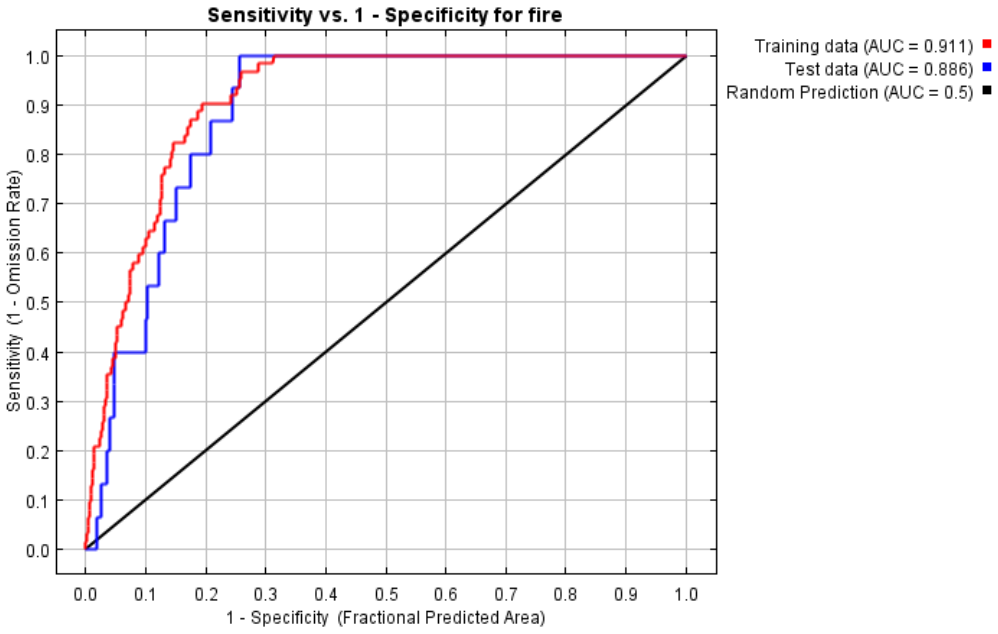


Figure 21. Receiver Operating Characteristic (ROC) curve for the wildfire model in 2005

The response curves clearly show the relationship of each environmental factor with wildfire probability in Tujiin Nars during May-July 2005 (Figure.22).

- The LST curve has a strong positive relationship with fire probability. Fire probability is near 0.0 at 18°C and steadily increases to nearly 0.9 when temperatures are between 35-38°C, demonstrating that extreme heat during May-July is a primary trigger for wildfires in Tujiin Nars.
- The Precipitation response curve is a well-defined and narrowly peaked curve. It increases sharply from 138-143 mm and reaches a maximum fire suitability of approximately 0.8 then sharply decreases in either direction. This shows that the fires in the area are limited to this specific range of moderate moisture and heat values that can ignite and spread a fire within Tujiin Nars.
- The Wind Speed response curve peaks narrowly at approximately 0.87-0.89 m/s (suitability 0.9). The curve rapidly declines at speeds over 0.92 m/s. This indicates that the more moderate wind speeds at these values allow the most optimal spread of fire throughout the region.
- The Slope response curve has its peak fire probability at near-flat terrains (0-2, suitability 0.9), and decreases quickly beyond 5. At over 15 slope, the curve drops to near zero fire probability. This indicates that wildfires have a strong likelihood of occurring at Tujiin Nars on the gently rolling plains characteristic of open grassland and steppe terrain.
- The NDVI response curve has two strong peaks, one near values 0.20-0.30 (suitability 0.95), a moderate decline followed by a second moderate peak, and then sharp drop-off past 0.65. This pattern of response for vegetation density indicates the region was most prone to fire at two different vegetation densities: very sparse, dry vegetation, and moderately vegetated areas.
- The Elevation response curve peaks in the 700-900 m elevation range (suitability 0.7). It rapidly decreases above 1000 m and drops off entirely above 1200 m. This demonstrates the strong fire susceptibility in this moderate elevation range where dry steppe and forest-steppe vegetation are the predominant landscape type.

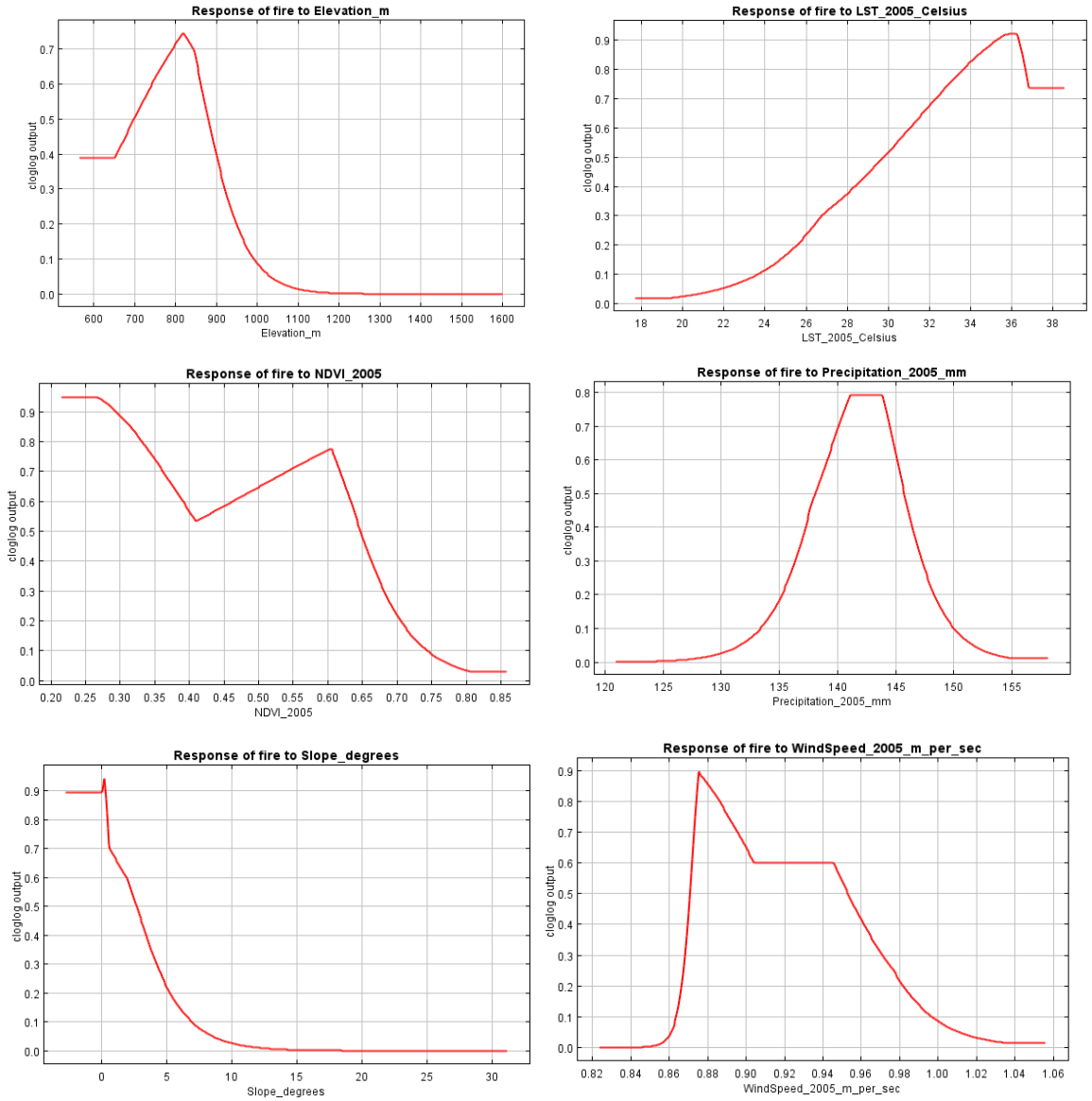


Figure 22. Response of wildfire occurrence to environmental variables in 2005

3.4.2.2 Performance of the Model and Environmental Variable Influence in 2007 (May-July)

The AUC value for the training dataset is 0.966, while the test dataset shows an AUC of 0.964. Both values are close to 1, demonstrating that the model has a very high ability to distinguish between fire-prone and non-fire-prone areas.

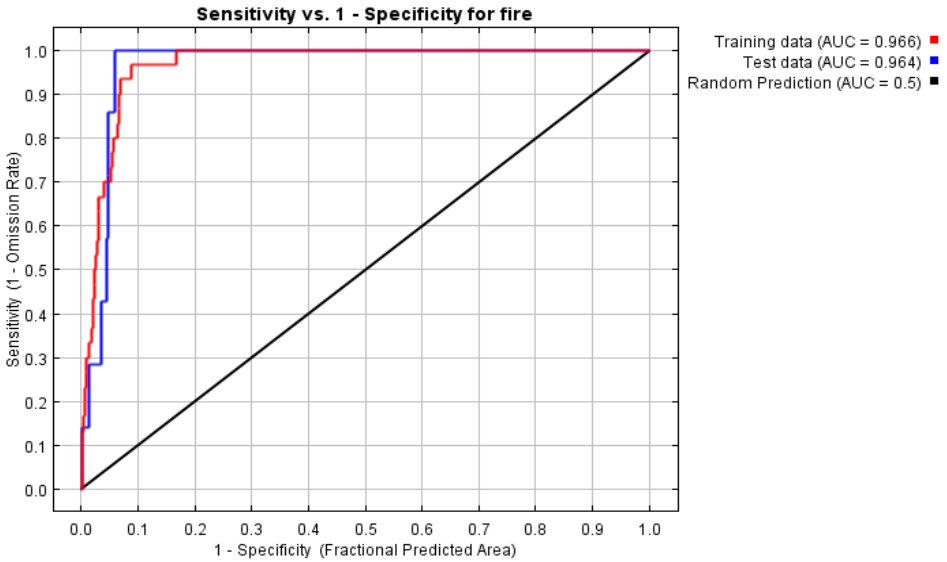


Figure 23. Receiver Operating Characteristic (ROC) curve for the wildfire model in 2007

Each relationship between environment variables and probability of wildfire occurrence in Tujiin Nars during May–July 2007 are revealed by the response curves (Figure.24).

- LST has a strong positive correlation, the probability of wildfire increases with the rise from near 0.0 at 20°C and reaches maximum suitability at 1.0 at 38-42°C. Extremely high land surface temperatures during the fire season of 2007 are the most significant conditions in Tujiin Nars.
- Precipitation has a gradually increasing response and rises from low probability at 170 mm to peak around 176-178 mm (suitability 0.5), and slightly decrease, which shows precipitation range at 2007 wildfire season are narrower and higher compared to the one at 2005, hence relatively moist background weather condition was present during the 2007 fire season.
- Wind speeds show a sudden increasing probability of wildfire occurrence above 1.00 m/s and reach suitability of 0.7 at 1.05-1.10 m/s, the steep rise in a narrower window. The optimal wind speed range during 2007 is noticeably higher than during 2005; it implies that wind conditions required to trigger fire spread are stronger in 2007 than in 2005.
- Slopes showed highest wildfire probability to occur at near-flat to mild slopes (0-5, suitability 0.9) but dropped to a very low value above 10, near 0 above 20. These patterns are consistent with the findings in 2005, suggesting that flat grassland and steppes are the most favorable habitat for wildfire occurrence in Tujiin Nars.
- NDVI has a clearly well-defined peak within the 0.40-0.50 vegetation index range (suitability 0.6-0.7) and decreases at both sides. Unlike the

pattern at 2005, the NDVI range of peaks are higher at 2007 than at 2005 which suggest moderate vegetation coverage is more associated with fire incidence at 2007 than at 2005.

- Elevation has a clearly defined peak between 700-800 m (suitability 0.8) and drop to a very low value above 900 m and near zero above 1000 m, The elevation range at 2007 wildfire season is narrow, indicating fire occurrence was more likely to occur at the low and mid elevation range of Tujiin Nars.

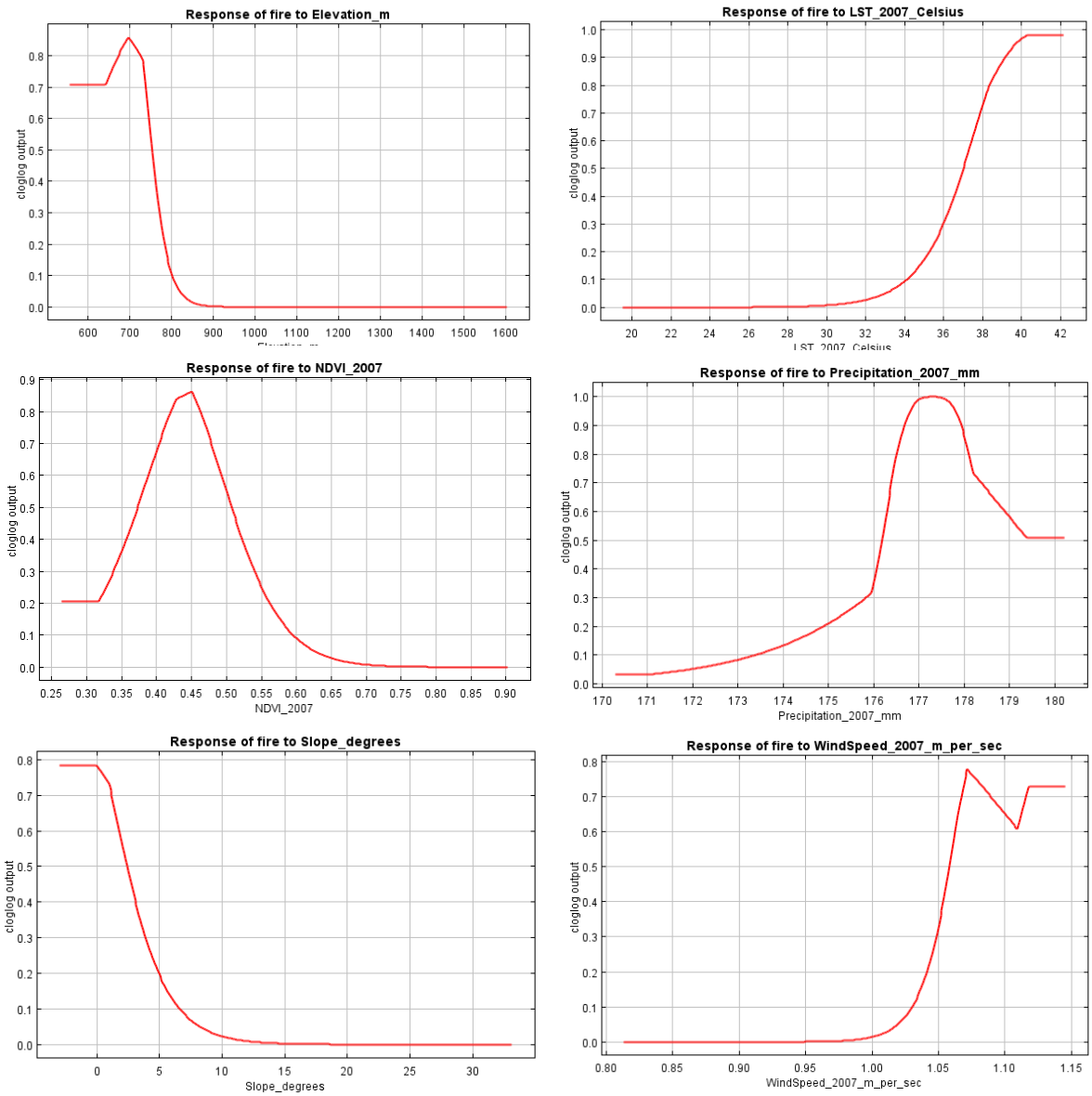


Figure 24. Response of wildfire occurrence to environmental variables in 2007

3.4.2.3 Performance of the model and environmental variable influence in 2025 (May-July)

The ROC curve for the Tujiin Nars 2005 May-July fire season model indicates high predictive accuracy (Figure.25). A training AUC value of 0.952 suggests that the model adequately describes the training data, while a test AUC value of 0.836 demonstrates adequate predictive accuracy when used on independent validation data.

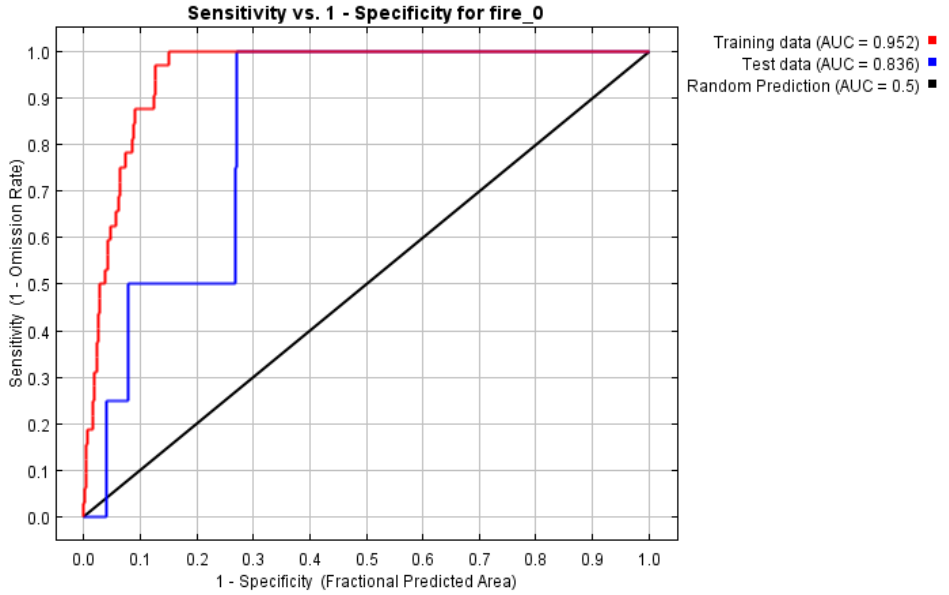


Figure 25. Receiver Operating Characteristic (ROC) curve for the wildfire model in 2025

The response curves illustrate the relationship between each environmental variable and wildfire probability in Tujiin Nars during May-July 2025 (Figure.26).

- Precipitation shows a unimodal response, with fire probability rising sharply from near 0.0 at 75 mm, peaking around 78-79 mm (suitability ~0.8), and declining steeply beyond 80 mm. This narrow optimal precipitation range suggests that the 2025 fire season occurred under highly specific and constrained moisture conditions.
- Slope exhibits the highest fire probability at near-flat to gently sloping terrain (0-3°, suitability ~0.8), declining sharply beyond 5° and approaching near zero above 15°, confirming that flat steppe and open grassland surfaces remain the most fire-prone landscape in Tujiin Nars.
- LST displays a well-defined bell-shaped response, rising from near 0.0 at 18°C and peaking around 27-28°C (suitability ~0.8), before declining symmetrically beyond 32°C. This indicates that moderate rather than extreme heat conditions were most strongly associated with fire occurrence in 2025.

- Wind Speed shows the sharpest and most dominant response, with fire probability reaching near 1.0 at 1.12-1.15 m/s and declining steeply beyond 1.18 m/s, approaching near zero above 1.25 m/s. This narrow but intense peak is consistent with Wind Speed's overwhelming dominance in the 2025 model (62.81% contribution), confirming that a specific threshold of wind intensity critically governed fire ignition and spread.
- NDVI displays a smooth unimodal peak centered around 0.50-0.55 (suitability ~0.9), declining symmetrically on both sides. This suggests that moderately vegetated areas with intermediate greenness were most susceptible to fire in 2025, likely reflecting partially dry but still fuel-rich vegetation conditions during the fire season.
- Elevation shows a sharp and narrow peak between 750–800 m (suitability ~0.85), declining steeply on both sides and approaching near zero above 950 m. This highly concentrated elevation response indicates that fire occurrence in 2025 was restricted to a specific altitudinal band, corresponding to the forest-steppe transition zone within Tujiin Nars.

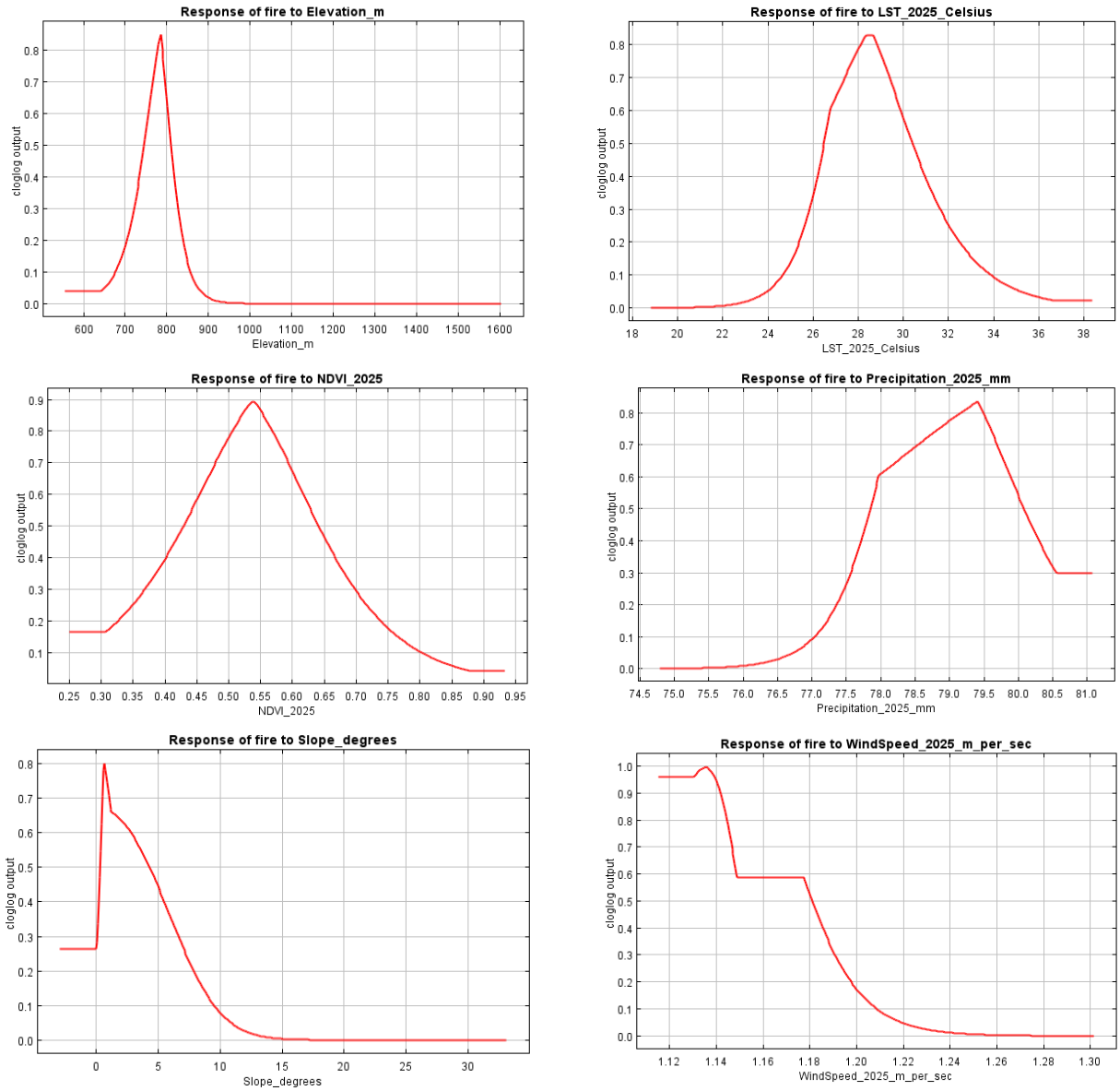


Figure 26. Response of wildfire occurrence to environmental variables in 2025

3.4.2.4 Comparison of environmental variable influence across 2005, 2007, and 2025 fire seasons in Tujiin Nars

The relative importance of Environmental variables governing fire risk in Tujiin Nars differed significantly between the three fire years. The relative contributions and permutations' importance showed varied dynamics from a seasonal to an inter-annual scale (Table.7).

In 2005 precipitation contributed 43.17%, permutation importance 48.59% and was the largest driver. This implies that the availability of moisture was the key driver of fire occurrence during the 2005 fire year. Its role decreased in 2007 (7.09%) but stayed constant in 2025 (21.89%).

The inter-annual shift in LST between 2005 and 2007 was striking; contribution dropped from 19.00% in 2005 to 84.31% in 2007, suggesting it was the single most dominant predictor for the 2007 fire year. Contribution decreased significantly in 2025 (1.67%) from 2007, suggesting an even greater shift between inter-annual fire risk factors.

Wind Speed showed an increasing contribution from 2005 (1.64%), to 2007 (6.10%), to become the most dominant predictor of fire risk in 2025 (62.81%, permutation importance 72.41%).

In 2005 slope was of a higher contribution (30.25%), and decreased in 2007 (0.72%) but rose again moderately in 2025 (9.02%). This suggests that topographic controls are likely to be important for spread but its influence is year specific and depends upon prevailing conditions.

NDVI, Aspect and Elevation did not significantly contribute across any of the fire years, all contributions being lower than 5%.

In summary the contribution analysis revealed distinct temporal shifts in dominant fire drivers: moisture-topographic controls dominated fire occurrence in the 2005 fire year; a distinct thermal control, extreme LST, governed fire risk in 2007 finally a shift towards wind as a dominant control of fire occurrence in the 2025 fire year. It could be that the climatic controls of fire risk are changing from a moisture to thermal driven system to a wind-driven one.

Table 7. Comparison of environmental variable importance for wildfire occurrence in Tujiin Nars (2005, 2007, 2025)

Variable	**Contribution, %**			**Permutation importance, %**		
	2005	2007	2025	2005	2007	2025
Elevation	0.49	0.19	0.93	3.83	0	9.44
LST	19	84.31	1.67	24.01	76.06	6.51
NDVI	1.13	0.28	2.58	3.49	0	0.75
Precipitation	43.17	7.09	21.89	48.59	13.18	0.27
Slope	30.25	0.72	9.02	18.19	1.38	10.43
WindSpeed	1.64	6.1	62.81	1.25	9.12	72.41

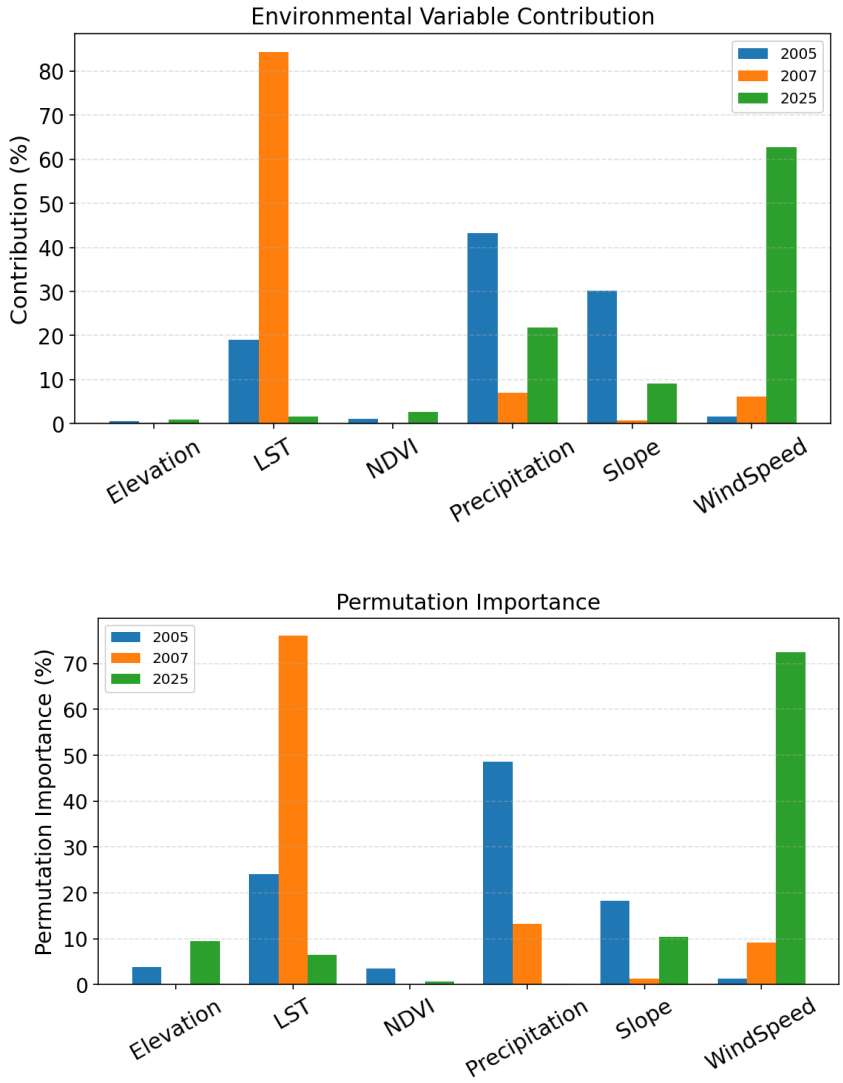


Figure 27. Comparison of environmental variable importance for wildfire occurrence in Tujiin Nars

Figure 27 shows five degrees of wildfire. Wildfire risk was distributed concentrated in east and northeast and low risk in west in all of the years, thus there is an obvious correlation with environmental gradients. This result coincides with the dominant variables result (Figure.28), and the distribution of wildfire risk was controlled by most dominant environmental variables like temperature, precipitation and wind in Tujiin Nars. In 2005, in regions with high risk and concentrated in the East, precipitation (43.17%) and slope (30.25%) were the most important contributing variables. Permutation importance also indicates that precipitation has the highest value (48.59%), which demonstrates that precipitation/moisture and topographic effects play important roles. In 2007, high risk spread to the center areas of the Tujiin Nars, land surface temperature is very important with high contribution (84.31%) and permutation importance (76.06%), this also demonstrates the effect of temperature that creates dryness, the most dominant factors are from temperature. However, In 2025, wildfire risk increased and concentrated

in eastern and central areas and became significant and intense, especially dominant with the value of wind speed (contribution is 62.81% and permutation importance is 72.41%), thus fire spread dynamic is the primary factor. However, NDVI and elevation variables have relatively low importance throughout all the years, implying that climate related factors have dominant effects on wildfire risk patterns.

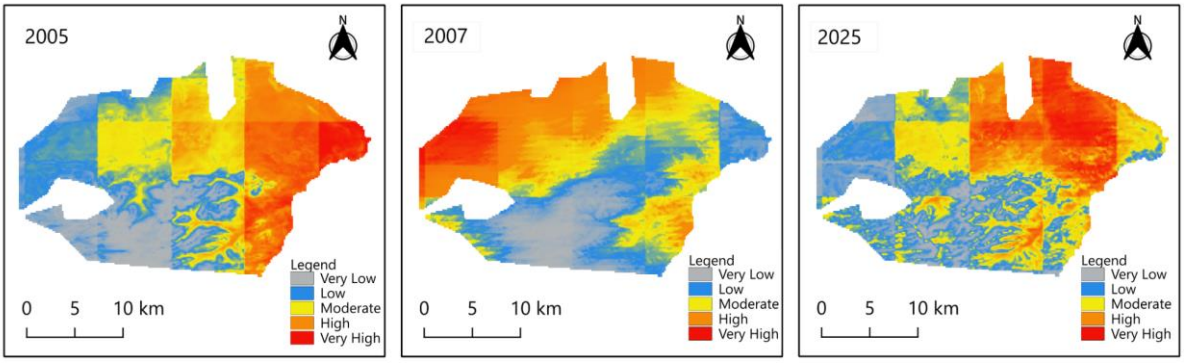


Figure 28. Wildfire risk distribution in Tujiin Nars for 2005, 2007, and 2025 derived from the MaxEnt model

3.5 Carbon emission

Table 8 presents a combined summary of the parameters used and the resulting burned area and CO_2 emissions for Tujiin Nars. The cumulative burned area for the selected years reached 166.39 km², with the majority (96.38%) occurring in grassland/steppe areas and only a small fraction (3.62%) in forest.

However, the distribution of carbon emissions shows an opposite pattern. Forest areas contributed 88.8% of total CO_2 emissions, while grassland accounted for only 11.2%, despite covering a much larger burned area. This is primarily due to the significantly higher fuel load in forest ecosystems compared to grassland.

The results indicate that wildfire impacts in Tujiin Nars are not directly proportional to burned area. Grassland fires dominate in spatial extent due to rapid spread across fine fuels, whereas forest fires, although more limited in area, generate substantially higher carbon emissions because of the combustion of dense ground-level biomass such as litter, dry needles, branches, and woody debris.

Table 8. Spatial distribution of carbon sequestration in Tujiin Nars for 2005, 2007, and 2025

Land cover	Fuel Load (kg/km²)	CC	EF (kg CO_2/kg)	Burned area (km²)	CO_2 emission (ton)	Contribution (%)
Forest	2,000,000	0.30	1.58	6.02	5,706.96	88.8
Grassland/Steppe	2,940	0.95	1.613	160.37	719.61	11.2

3.6 Carbon sequestration

Figure 29 illustrates the spatial distribution of carbon sequestration in Tujiin Nars for the years 2005, 2007, and 2025. The maps reveal clear spatial variability in carbon uptake across the study area, with lower values (red-orange) representing areas of reduced vegetation productivity and higher values (blue-green) indicating greater carbon absorption.

In 2005, lower sequestration values are predominantly observed in the northern and northeastern parts of the study area, suggesting limited vegetation productivity and possible effects of disturbance. A similar pattern is observed in 2007, although slight improvements in sequestration are visible in some central regions, indicating early stages of vegetation recovery.

By 2025, a noticeable increase in sequestration is evident across much of the area, particularly in central and southern regions where higher values dominate. This spatial shift toward increased carbon uptake reflects improved vegetation condition and enhanced ecosystem productivity over time.

The observed patterns are consistent with the statistical results, where mean carbon sequestration increased from 4.80 ton C/ha in 2005 to 6.26 ton C/ha in 2025, and total sequestration rose from 340,251.89 tons to 443,327.84 tons. These results indicate that vegetation recovery following wildfire disturbance has contributed to a gradual increase in carbon uptake capacity.

Overall, the maps demonstrate that although wildfire initially reduces vegetation productivity, the Tujiin Nars ecosystem shows strong recovery potential. The increasing sequestration values over time suggest that post-fire regeneration plays a key role in restoring ecosystem functions and maintaining long-term carbon balance.

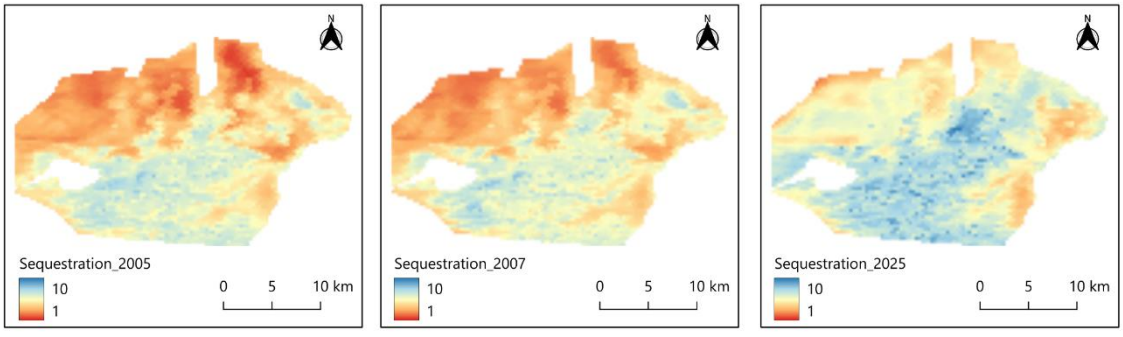


Figure 29. Carbon sequestration capacity of Tujiin Nars across wildfire years (2005, 2007, and 2025)

Conclusion

The thesis revealed that the occurrence of wildfire in Selenge Province and Tujiin Nars exhibit distinct temporal, spatial and environmental characteristics within 2001–2025, and most wildfires concentrated during the warm season, particularly spring and early summer. A total of 605 fires detections and 7,809.29 km2 burned area were obtained for Selenge Province during 2001-2025, and 2009 was found as peak fire year, and only 3 fire events were detected within Tujiin Nars in 2005, 2007 and 2025. This study proves that fire occurrence is a complex interaction process dominated by climate, vegetation, terrain, human activity in the study area.

The spatial distribution showed that fire did not occur randomly in the area but accumulated in vulnerable areas, fire hotspots in Selenge Province was mainly found in northern, northeast and east forest areas, and those hot areas in Tujiin Nars which had high recurrence located in northern, northeast and east part of nature reserve area, due to influences of ecotones (forest-steppe ecotone), fuel availability, land cover, terrain, and human accessibility. The index of Wildfire Risk showed that highest risk values are concentrated in the area where dense vegetation coverage and the landscape were suitable in terms of topography and accessible road in Tujiin Nars nature reserve.

The predictive accuracy for the models, based on MaxEnt, was proved and the key determinants of wildfires were confirmed to change over time. For Selenge Province, land surface temperature and precipitation were important predictors in spring fire occurrence, but wind speed become the most important factors in autumn fire event. Meanwhile, moisture and terrain conditions were the primary factors controlling the occurrence of the 2005 fire event in Tujiin Nars nature reserve, and temperature of extreme heat dominated the fire occurrence in 2007 fire events, but wind speed becomes the most important factor with contribution and permutation importance as highest for the 2025 fire event. So it seems that occurrence of wildfires will be more vulnerable with the changing conditions in the future.

Based on carbon calculation results, impact on ecosystem function even limited area burned was also profound. In Tujiin Nars, 96.38% of burned area were grassland-steppe, but its CO2 emission was only 11.2% while fire occurrence was 88.8% of total CO2 emission from the forests, because of higher biomass and fuel load of the forest ecosystem than grassland-steppe ecosystems, total CO2 emission during fire events reached 6,426.57 tons with 5,706.96 tons CO2 from the forests. Post-fire carbon sequestration showed significant recovery capability; mean sequestration rate increased from 4.80 t C/ha in 2005 to 6.26 t C/ha in 2025, and total sequestration rate increased from 340,251.89 t to 443,327.84 t.

In conclusion, Tujiin Nars is a vulnerable forest-steppe ecosystem prone to fire risk, both CO2 emission and subsequent carbon sequestration were significant, the fire risk, emission and recovery capacity are closely related. Fire prevention measures must focus on the highest risk area especially areas with proximity to road and areas with good conditions regarding vegetation and terrain. The rehabilitation measure and long-term monitoring are also crucial for maintaining the ecosystem carbon sequestration capacity.

Reference

1. Bao, Y., Shinoda, M., Yi, K., Fu, X., Sun, L., Nasanbat, E., et al. (2022). Satellite-based analysis of spatiotemporal wildfire pattern in the Mongolian Plateau. *Remote Sensing, 15*(1), 190. https://doi.org/10.3390/rs15010190
2. Shen, Z., Giljohann, K., Liu, Z., Pausas, J., & Rogers, B. (2025). Novel wildfire regimes under climate change and human activity: patterns, driving mechanisms and ecological impacts. *Philosophical Transactions of the Royal Society B, 380*(1924). https://doi.org/10.1098/rstb.2023.0446
3. Jargal, J. (2003). Protected area status in Mongolia. *Mongolian Journal of Biological Sciences, 1*(2), 49–54.
4. Bedunah, D. J., & Schmidt, S. M. (2004). Pastoralism and protected area management in Mongolia's Gobi Gurvansaikhan National Park. *Development and Change, 35*(1), 167–191. https://doi.org/10.1111/j.1467-7660.2004.00347.x
5. Selenge aimag's efforts to expand forests. MONTSAME News Agency.
6. Tujiin Nars saved from extinction. MONTSAME News Agency.
7. IDGN-1.-NEAFF_Park-Byungbae_Mongolian-Forest-Restoration-Project-compressed. (n.d.).
8. Mongolian Statistical Information Service. (2025).Wildfire statistical data of Mongolia 1212.mn
9. National Emergency Management Agency. (2025). Forest wildfire damage information in Selenge province
10. Altangerel, M.-E., Damdinsuren, A., Enkhtuya, J., & Erdenebaatar, N. (2021). Forest fire risk assessment model using remote sensing and GIS techniques in Tujiin Nars National Park, Mongolia. *Proceedings of the Mongolian Academy of Sciences, 61*(2), 10–19.
11. Nasanbat, E., Lkhamjav, O., Bulkhbai, A., Tsevee-Oirov, C., Mishigdorj, O., & Magsar, E. (2017). A fire risk map for protected areas of Mongolia: Tujiin Nars NP, Khan Khentii SPA and Bogd Khan SPA. *International Journal of Wildland Fire, 26*(8), 669–681.
12. Giglio, L., Boschetti, L., Roy, D. P., Humber, M. L., & Justice, C. O. (2018). The Collection 6 MODIS burned area mapping algorithm and product. *Remote Sensing of Environment, 217*, 72–85. https://doi.org/10.1016/j.rse.2018.08.005
13. Gorelick, N., Hancher, M., Dixon, M., Ilyushchenko, S., Thau, D., & Moore, R. (2017). Google Earth Engine: Planetary-scale geospatial analysis for everyone. *Remote Sensing of Environment, 202*, 18–27. https://doi.org/10.1016/j.rse.2017.06.031

14. Yang X, Jin X, Zhou Y. Wildfire risk assessment and zoning by integrating Maxent and GIS in Hunan province, China. Forests. 2021 Sep 23;12(10):1299.
15. Phillips SJ, Dudík M. Modeling of species distributions with Maxent: new extensions and a comprehensive evaluation. Ecography. 2008 Apr;31(2):161-75.
16. Elith, J., Phillips, S. J., Hastie, T., Dudík, M., Chee, Y. E., & Yates, C. J. (2011). A statistical explanation of MaxEnt for ecologists. *Diversity and Distributions, 17*(1), 43–57. https://doi.org/10.1111/j.1472-4642.2010.00725.x
17. Phillips, Steven. A Brief Tutorial on Maxent. 2017.
18. IPCC. (2006). *2006 IPCC Guidelines for National Greenhouse Gas Inventories, Volume 4: Agriculture, Forestry and Other Land Use.* Intergovernmental Panel on Climate Change, IGES, Japan. https://www.ipcc-nggip.iges.or.jp/public/2006gl/vol4.html
19. Casady, G. M., van Leeuwen, W. J. D., & Marsh, S. E. (2013). Monitoring the effects of forest restoration treatments on post-fire vegetation recovery with MODIS multitemporal data. *Sensors, 8*(3), 2017–2042. https://doi.org/10.3390/s8032017
20. Casady, G. M., van Leeuwen, W. J. D., & Marsh, S. E. (2013). Monitoring the effects of forest restoration treatments on post-fire vegetation recovery with MODIS multitemporal data. Sensors, 8(3), 2017–2042. https://doi.org/10.3390/s8032017
21. Enkhbold E. Spatiotemporal patterns of wildfires and estimation of carbon emissions and carbon sequestration in eastern Mongolia. [Mongolia]: GMIT; 2025.

Appendix

```
// Monthly Burned Area in Selenge (2000–2025)
var provinces = ee.FeatureCollection("FAO/GAUL/2015/level1")
  .filter(ee.Filter.eq('ADM0_NAME', 'Mongolia'));
var selenge = provinces.filter(ee.Filter.eq('ADM1_NAME', 'Selenge'));
Map.centerObject(selenge, 7);
Map.addLayer(selenge, {color: 'red'}, 'Selenge');
// MODIS Burned Area (BurnDate band)
var burned = ee.ImageCollection("MODIS/061/MCD64A1")
  .filterDate('2000-01-01', '2025-12-31')
  .select('BurnDate')
var years = ee.List.sequence(2000, 2026);
var months = ee.List.sequence(1, 12);
var monthlyBurned = ee.FeatureCollection(
  years.map(function(year) {
    year = ee.Number(year);
    return months.map(function(month) {
      month = ee.Number(month);
      var start = ee.Date.fromYMD(year, month, 1);
      var end = start.advance(1, 'month');
      var ic = burned.filterDate(start, end);
      var burnedAreaKm2 = ee.Image(
        ee.Algorithms.If(
          ic.size().gt(0),
          ic.map(function(img) {
              return img.gt(0).rename('BurnDate'); // burned pixels as 1
            })
            .sum()
```

```
            .multiply(ee.Image.pixelArea())
            .divide(1e6) // km²
            .rename('BurnDate'),
          ee.Image(0).rename('BurnDate')   )     );
      var stats = burnedAreaKm2.reduceRegion({
        reducer: ee.Reducer.sum(),
        geometry: selenge.geometry(),
        scale: 500,
        maxPixels: 1e13
      });
      return ee.Feature(null, {
        'year': year,
        'month': month,
        'burned_km2': ee.Number(stats.get('BurnDate'))
      });
    });
  }).flatten()
)
print('Monthly Burned Area (km²) - Selenge 2000–2025', monthlyBurned);
```